

RI 9583

RI 9583

REPORT OF INVESTIGATIONS/1995

**For Reference**

Not to be taken from this room

## Use of a Tracer for In Situ Stope Leaching Solution Containment Research

UNITED STATES DEPARTMENT OF THE INTERIOR

UNITED STATES BUREAU OF MINES



*U.S. Department of the Interior*  
*Mission Statement*

As the Nation's principal conservation agency, the Department of the Interior has responsibility for most of our nationally-owned public lands and natural resources. This includes fostering sound use of our land and water resources; protecting our fish, wildlife, and biological diversity; preserving the environmental and cultural values of our national parks and historical places; and providing for the enjoyment of life through outdoor recreation. The Department assesses our energy and mineral resources and works to ensure that their development is in the best interests of all our people by encouraging stewardship and citizen participation in their care. The Department also has a major responsibility for American Indian reservation communities and for people who live in island territories under U.S. administration.

**Report of Investigations 9583**

## **Use of a Tracer for In Situ Stope Leaching Solution Containment Research**

**By Nadia C. Miller and Carl H. Schmuck**

**UNITED STATES DEPARTMENT OF THE INTERIOR  
Bruce Babbitt, Secretary**

**BUREAU OF MINES  
Rhea Lydia Graham, Director**

---

This report has been technically reviewed, but it has not been copy edited because of the closure of the agency.

## CONTENTS

	<i>Page</i>
Abstract . . . . .	1
Introduction . . . . .	1
Test site description . . . . .	2
Regional geology . . . . .	4
Regional hydrology . . . . .	5
Rock mass characterization . . . . .	7
Geological characterization . . . . .	7
Geophysical characterization . . . . .	7
Hydrology . . . . .	8
Tracer tests . . . . .	8
Tracer observations . . . . .	10
Borehole 6 . . . . .	11
Borehole 7 . . . . .	12
Borehole 3 . . . . .	12
Borehole 4 . . . . .	13
Constant-head test . . . . .	13
Borehole 3 . . . . .	15
Borehole 4 . . . . .	16
Borehole 6 . . . . .	16
Borehole 8 . . . . .	16
Borehole 10 . . . . .	16
Summary and conclusions . . . . .	17
Acknowledgments . . . . .	18
References . . . . .	19

## ILLUSTRATIONS

1. Schematic of stope leaching process . . . . .	22
2. Plan view of the solution control site . . . . .	23
3. Longitudinal section of site . . . . .	24
4. Orientation of mapped fractures in the stope . . . . .	25
5. Tracer test levels and concentrations . . . . .	26
6. Tracer level in the stope during test 1 . . . . .	27
7. Conductivity in the stope during test 1 . . . . .	28
8. Borehole 6 conductivity during test 1 . . . . .	29
9. Borehole 6 conductivity during test 2. . . . .	30
10. Borehole 6 conductivity during test 3.. . . .	31
11. Borehole 3 conductivity during test 2. . . . .	32
12. Borehole 3 conductivity during test 3.. . . .	33
13. Tracer level in the stope during test 3.. . . .	34
14. Borehole 4 conductivity during test 3.. . . .	35
15. Tracer level in stope during constant head test . . . . .	36

## ILLUSTRATIONS—Continued

		<i>Page</i>
16.	Borehole 3 conductivity - constant head test . . . . .	37
17.	Borehole 4 conductivity - constant head test . . . . .	38
18.	Borehole 6 conductivity - constant head test . . . . .	39
19.	Borehole 8 conductivity - constant head test . . . . .	40
20.	Borehole 10 conductivity - constant head test . . . . .	41
21.	Stope conductivity during constant head test . . . . .	42
22.	Draining profiles from stope . . . . .	43

## TABLE

1.	Tracer test results . . . . .	21
----	-------------------------------	----

## UNIT OF MEASURE ABBREVIATIONS USED IN THIS REPORT

cm	centimeter(s)
cm/s	centimeter(s) per second
h	hour(s)
kHz	kilohertz
km	kilometer(s)
L	liter(s)
L/min	liter(s) per minute
m	meter(s)
min	minute(s)
mm	millimeter(s)
pct	percent
ppm	parts per million
W	watt(s)
μS/cm	microSiemen(s) per centimeter

# USE OF A TRACER FOR IN SITU STOPE LEACHING SOLUTION CONTAINMENT RESEARCH

By Nadia C. Miller<sup>1</sup> and Carl H. Schmuck<sup>2</sup>

---

## ABSTRACT

In situ stope leaching is an innovative mining system that reduces the surface impacts of conventional underground mining. As in any leaching operation, stope leaching requires hydrologic site characterization and control of leaching solutions. Several tracer tests, using sodium chloride (NaCl) in various concentrations, were conducted by the U.S. Bureau of Mines (USBM) in an underground experimental stope to simulate a leaching environment.

The tests were conducted in fractured crystalline rock that was partially water-saturated. As tests progressed, the surrounding fractures became more saturated. A predominant flow direction away from the stope was found during testing. Testing procedures, results, and a remediation plan for in situ leaching based on field observations are presented in this report.

## INTRODUCTION

Conventional underground mining involves the excavation and transportation of ore to the surface for processing. Tons of solid material are extracted from underground mining systems to produce kilograms, and sometimes only grams, of final product. Surficial processing of ore results in the disposal of most of the excavated material on the surface. Long term degradation by wind and water can result from surface disposal which may cause acid rock drainage or other conditions that adversely impact the environment.

The U.S. Bureau of Mines (USBM) is currently investigating in situ recovery of minerals. As a part of this initiative, research in "Stope Leaching" is being conducted to modify conventional mining practices by significantly reducing the amount of material brought to the surface.

The underground stope leaching mining system involves recovering low-grade reserves by applying leach solutions to fragmented mineralized rock that has been blasted in place, or backfilled into empty stopes. If blasted, only enough material is

---

<sup>1</sup>Geological engineer, Denver Research Center, U.S. Bureau of Mines, Denver, CO.

<sup>2</sup>Mining engineer, Denver Research Center (now with Mine Health and Safety Administration, Ground Support Division, Denver, CO)

removed from the underground mining area (stope) to allow for adequate expansion during the blasting, reducing the amount of material brought to the surface by at least two-thirds. After blasting, leach solutions containing chemical solvents and/or bacteria are circulated through the fragmented ore to dissolve the desired mineral (figure 1). The resulting mineral-rich solution (pregnant leach solution) is pumped to a processing facility where the product is removed, and the leach solution is regenerated for reuse underground.

Successful implementation of stope leaching requires effective solution management. Effective solution management requires the containment of leach solutions within the leaching stope and the limitation of external groundwater flow into the stope. Loss of leach solutions to the surrounding rock mass has environmental and economic implications. Loss of pregnant leach solution results in lost revenue from costs incurred with no product gained. Leaching solution lost to the rock mass may also degrade adjacent ground water quality. Water flowing into a leaching stope can sufficiently dilute the leaching solution. Water may also reduce mineral dissolution in the stope and make recovery of the dissolved mineral unattainable at the processing facility.

Characterization of the rock mass prior to leaching is critical to effective solution management. Detailed rock mass characterization located zones of high permeability that could require sealing before leach solutions are introduced to the stope. USBM researchers have tested and compared rock mass characterization methods utilizing geologic mapping, geophysical techniques, and hydrologic procedures at an underground test facility in the Edgar Mine (an experimental mine in Idaho Springs, CO), which is owned and operated by the Colorado School of Mines (CSM). Hydrologic procedures, including packer tests, were conducted before and after stope excavation (Miller, 1993). This earlier research was essential for the design and interpretation of data of tracer test studies. Several tracer tests, using NaCl, were conducted in the underground test stope to simulate solution movement during leaching. The tracer test procedures and results are presented.

## TEST SITE DESCRIPTION

The project site is located at the Edgar Mine (in Sec. 26 and 35, T. 35 N., R. 73 W.), approximately 0.4 km north of Idaho Springs, CO. Hydrologic testing was conducted at an underground stope site located approximately 300 m from the Miami Tunnel portal of the mine at an approximate elevation of 2,400 m above sea level. The test facility is approximately 180 m below the ground surface.

The test facility was constructed by extracting rock from a stope using a blasting technique designed to maximize ore fragmentation while minimizing damage to the wall rock. The technique is sometimes referred to as smooth-wall blasting where the outer perimeter of the blast hole pattern is drilled on a closer spacing between holes.

Explosive is only loaded in every other hole in this outer perimeter. In addition, the blast holes that are loaded in the outer perimeter receive less explosive than the other holes in the pattern. The stope was excavated between the extension of an existing lower drift and an upper chamber. Total height of the stope is 8.2 m, including the drift. The rock excavated between the lower drift and the upper chamber (5.8 m) was blasted in a circular configuration with a nominal diameter of 1.8 m (figure 2). Boreholes (7.62 cm and 10.16 cm diam) were drilled at intervals beneath and around the outside perimeter of the stope for core sampling and characterization of the rock mass. These boreholes then became monitoring locations during the tracer tests (figures 2 and 3).

A reinforced concrete bulkhead was constructed in the bottom access drift to contain water in the stope (figure 3). The concrete (35.6 cm thick) was reinforced with two mats of No. 6 reinforcing steel on 30.5-cm vertical and 50.8-cm horizontal centers. Bulkhead anchorage was provided by drilling holes 10 cm deep into the rock along each side of the bulkhead and grouting the rebar into the holes. Wet concrete was dropped from the upper stope chamber through a 15-cm-diam borehole into the concrete forms below. The concrete, containing super plasticizer, was vibrated through access panels in the forms to ensure consistency and contact with the surrounding rock (Lutzens, 1994).

A solution delivery and recovery piping system was constructed (figure 3) to complete the simulated leaching stope as a test facility for hydrology research using tracers. This solution handling system consisted of pipe networks, pumps, valves, flow meters and solution reservoirs. Three subsystems comprise the total system: (1) main city water inflow source, (2) tracer mixing and delivery system, and (3) bulkhead seepage collection and return system.

The main stope inflow was provided by a 3.8-cm inner diameter (ID) PVC pipe through which the mine pumps could provide up to 380 liters per minute (L/min) directly from the city water lines or an underground mine reservoir with a capacity of 61,000 liters (L) of city water. A check valve was installed in the stope inflow line so that no back flow of water and/or tracer would reach the main mine water distribution system.

A piping and pumping subsystem was designed to add a concentrated tracer solution to the main inflow pipe at a constant rate. The continuous addition of a concentration tracer flow throughout the stope flooding period eliminated the potential bias in data from mixing the tracer in the stope after it was filled with water. The tracer subsystem used two 200-L plastic drums with gravity feed into a plastic column in which a low-flow, rheostat-controlled, submersible pump was installed. NaCl was mixed with water in the plastic drums at a higher concentration calculated to match the overall flow rate into the stope and achieve the desired tracer test concentration throughout stope flooding. A plastic tube, 1.3 cm ID, was connected between the



tracer pump and the 3.8-cm main pipeline. A second check valve was installed in the tracer feed tube to avoid back pressure leakage from the main line.

Although seepage around the bulkhead was reduced by a factor of 100 with surface grouting of fractures and seeps inside the stope, a collection and recovery system was constructed for the remaining 0.38 to 1.25 L/min that seeped around the bulkhead. This collection and return system consisted of a trench excavated at the outside of the bulkhead base, an electric marine sump pump in the trench, and a rubber-lined collection sump (10,000 L capacity). The collection sump could be pumped with a 2-hp centrifugal pump equipped with manual and remote electrical operation. In addition, two black plastic pipelines were connected between outlets in the bulkhead and the 10,000-L collection sump for emergency solution drainage from the stope.

Instrumentation to measure and control the quantity of flow and flow rate in the solution delivery system consisted of a large flow meter with dial and electrical readout in the main inflow pipeline, a small flow meter with dial and electrical readout in the tracer delivery tube, a flow meter with dial readout in the discharge line from the centrifugal pump at the 10,000-L collection sump, and a flow meter with dial in the mine emergency dump line from the bulkhead to the collection sump. The electrical readouts from the main inflow meter and the tracer feedline meter were connected to a computer that was converted to a data logger with screen display. This real-time screen display of flow rates was used to manually adjust inflow valve settings on the main water line to the stope and rheostat adjustments on the tracer injection pump to maintain consistent tracer concentrations as the stope was flooded.

### Regional Geology

The Edgar Mine is located within the Colorado Front Range, a geological region that has been affected by seven structural events dating back 1.75 billion years (Hutchinson, 1983). The predominate rock types in the area are Precambrian metamorphosed sedimentary rocks of the Idaho Springs Formation, metamorphosed igneous rocks, and igneous rocks. Predominant rock types at the test site include banded quartz biotite gneiss, granitic pegmatite, and biotite hornblende schist. Gangue minerals include biotite, quartz, feldspars, hornblende, chlorite, and pyrite. Clay occurs in fault gouge zones or zones of high alteration. The presence of iron oxidation in some fracture surfaces indicates the occurrence of past movement of fluids.<sup>3</sup> The mine is located on the steeply dipping northwest flank of the Idaho Springs anticline. This anticline is asymmetric and trends approximately N. 55° E.

---

<sup>3</sup>Speirer, R. A. and N. C. Miller. Geologic Rock Mass Characterization for Underground In-Stope Leaching. Presentation to Alaska Miners' Association, Nov. 1992.

The Idaho Springs fault, trending N. 60° W, is 0.4 km southwest of the mine. Most of the faults in the area are Tertiary in age (2 to 12 million years ago) and generally follow preexisting planes of weakness in the Precambrian rocks (Harrison and Moench, 1961). Five smaller faults were mapped in the drifts surrounding the test stope. Three of the faults strike N. 20° E, one strikes N. 40° E, and one strikes N. 30° W. None of these faults intersect the stope because they are oriented away from the stope.<sup>4</sup>

### Regional Hydrology

Groundwater present in the Idaho Springs area is primarily found in fractures of igneous and metamorphic rock. Effective porosities of the regional rock are relatively low and have been measured to range from  $1 \times 10^{-2}$  to  $1 \times 10^{-3}$  pct (INTERA, 1983). Effective porosities in similar crystalline rocks in the region range from  $1 \times 10^{-1}$  to  $4 \times 10^{-5}$  percent for depths of 20 m and  $2 \times 10^{-1}$  to  $4 \times 10^{-8}$  percent for depths of 50 to 200 m (Snow, 1968b and 1969). The hydraulic conductivity of the rocks found in the Edgar Mine has ranged from  $9.9 \times 10^{-10}$  cm/s to  $9.9 \times 10^{-2}$  cm/s.<sup>5</sup> Snow (1968b) found regional hydraulic conductivities in similar rocks to range between  $3.53 \times 10^{-6}$  cm/s to just over  $3.53 \times 10^{-4}$  cm/s. Water slug tests performed for this study found the average hydraulic conductivity for wall rock to range between  $1 \times 10^{-5}$  cm/s to  $4.1 \times 10^{-3}$  cm/s (Miller, 1993).

Fractured aquifers in the area have been estimated to be between 61 and 107 m in depth (Snow, 1968a; Florquist, 1973). Because the permeability of these water-bearing fracture zones decreases with depth, it is believed that greater than 90 percent of the Idaho Springs aquifer permeability is within 24 m of the surface.<sup>6</sup> The water table of this aquifer rises and falls considerably with climatic variations. The regional water table in this aquifer is located between 46 and 61 m below the ground surface (Moench and Drake, 1966) and between 15 and 53 m where the topography is gently

---

<sup>4</sup>Work cited in footnote 3.

<sup>5</sup>Montazer, P. Permeability of Unsaturated, Fractured Metamorphic Rocks Near an Underground Opening. Ph.D. Dissertation, Nov. 1982, CO. Sch. of Mines, Golden, CO, T-2540, 447 pp.

<sup>6</sup>Camp Dresser and McKee, Inc., Supplemental Data on Tunnels, Clear Creek/Central City Site. Letter Report, Project 2684 for Gormley Consultants Inc., CO., Oct. 1988, 13 pp; available from Superfund Records Cent., EPA, Region VIII, Denver, CO.

sloping.<sup>7</sup> However, the regional water table has been artificially lowered within the past 100 years due to mine workings that provide deep drainage.

Due to the excavation of the Big Five Tunnel in the early 1900's for drainage and ore haulage purposes at a lower elevation, the Edgar Mine was dewatered. As a result, most of the rock mass in the mine is unsaturated; however, there are fractures that transport water through the mine.

Locally, the hydraulic gradient appears to be controlled by the regional structural geology and vein structure, rather than the topography. Wells on the Edgar property, which were installed by the U.S. Army Corps of Engineers, show that the piezometric surface in the wells parallels the majority of the attitudes of joints, measured adjacent to the wells.<sup>8</sup> From the structural data collected at the mine, the direction of the hydraulic gradient was estimated to be N. 6° W. This direction is not detectable at the experimental site because of the relatively small scale of the site. Water levels have been monitored in the boreholes surrounding the stope for 4 years. The water levels vary in these boreholes from 0 to several tens of centimeters. There is no pattern that shows a definite hydraulic gradient. There also is no water level trend associated with precipitation events. This may be due to the fact that flow in the rock mass is primarily controlled by a few fractures, and that these fractures do not have a high degree of connectivity.

Geologic and hydrologic data were coupled with modeling to evaluate the migration of a leaching solution plume. PLUME (In Situ, Inc., 1986), an analytical computer model based on a continuum fracture flow approach<sup>9</sup> was thought to best support the geologic characteristics associated with the project, even though saturated conditions were assumed when using the model. The model predicted that an escaping lixiviant plume would travel in a westerly direction. The model results are acceptable up until the plume intercepted a fault or mineralized vein. These features would

---

<sup>7</sup>Camp Dresser and McKee, Inc., Feasibility Study Report, Operable Unit No. Three, Argo Tunnel Discharge Control. Aug. 1989, U.S. EPA Contract No. 68-01-6939.

<sup>8</sup>Cameron, R., Investigation and Geophysical Testing on Excavation of a Tunnel Test Site Under BRRDEC Tunnel Detection Program. Unpublished Report for U.S. Army, Belvoir Res., Dev., and Eng. Cent. Dep. Min. Eng., CO Sch. Mines, Golden, CO, 1987, 32 pp.

<sup>9</sup>de Josselin de Jong, G. and Shao Chih Way., Dispersion in Fissured Rock. N.M. Inst. of Min. and Technol., Socorro, 1972, 30 pp.

probably direct the plume in a northwesterly direction toward the Big Five Tunnel, since the tunnel drains the Edgar mine workings.

## ROCK MASS CHARACTERIZATION

Rock surrounding the leaching stope was used for the walls of the leaching vessel that contained both the fragmented ore and the leach solutions. Characterizing the rock prior to leaching is essential for locating fractures, faults, and other potential zones of solution migration. Rock mass characterization research at the Edgar Mine was focused on the block of rock between the upper and lower levels of the underground test stope and in a zone immediately beneath the stope (figure 3).

Research at the Edgar Mine test site investigated the hydrogeologic processes involved in solution loss and the effectiveness of different techniques for characterizing these processes. Rock mass characterization was conducted in three phases: preblast rock characterization, postblast rock characterization, and hydrologic prediction. Rock mass characterization of the stope was facilitated by logging core for fractures from the holes drilled for stope blasting and from eight borehole monitoring wells drilled beyond the outside perimeter of the stope (figure 2). Figure 4 shows the orientation of fractures mapped inside the stope after blasting occurred.

Results of rock mass characterization research at the Edgar stope are discussed in the following sections.

### Geological Characterization

Thorough geologic mapping was conducted along approximately 350 horizontal meters of drifts, 14 vertical meters of the ventilation raise in the vicinity of the simulated leaching stope, and the stope itself. Fracture orientations (apparent strike and dip), fracture spacings, fracture lengths, and fracture surface oxidation and roughness were noted. Approximately 61 m of oriented core was obtained from six holes (four vertical, and two inclined) in the area of the simulated stope. Fracture orientations and other characteristics from drift mapping and core logging were submitted to statistical analysis.

### Geophysical Characterization

Geophysical testing was conducted in the boreholes to delineate open fractures or fracture zones that may transmit solution from the stope. Geophysical data were generated using single-hole techniques including natural gamma, spontaneous potential, resistivity, single-point resistance, neutron, compensated density, sonic, and single-well electrical tracer (SWET) tests. Additional data were obtained by conducting high-frequency cross-hole seismic tomography. The geophysical data were then compared with the fracture and lithologic core data.

Examination of the various single-hole geophysical logs showed mixed results when compared to core logs. Open fractures and sites of water loss were most effectively indicated by the sonic velocity and single-point resistance logs. Natural gamma, neutron, and compensated density logs would indicate changes in lithology. However, no specific single-hole technique consistently responded to probable, even known, zones of solution loss (Boreck and Goris, 1992).

Preblast cross-hole seismic testing was conducted for five borehole combinations. The cross-hole system consisted of a 20 kHz piezoelectric energy source and receiver system with a digital storage oscilloscope for waveform acquisition and storage. The waveform data were analyzed using tomographic computer software. The software generated a display of the energy ray paths created by sonic pulses in one borehole and received in another borehole. Many of the fracture zones causing water loss coincided with low velocity zones (Jessop et. al., 1994).

### Hydrology

The regional hydrologic system was found to be influenced by the geologic structure of the region. Fractures, on a local scale, and natural and manmade discontinuities, on a regional scale, were believed to be instrumental in directing fluid flow within the rock mass (Miller, 1993). To evaluate hydraulic fracture properties, hydraulic conductivities of the fractures adjacent to and at the stope room were obtained using both air and water slug tests. Although a large range of hydraulic conductivities were obtained from this testing, an average hydraulic conductivity of  $2.3 \times 10^{-2}$  cm/s was used for input into a computer model for evaluation of flow within the rock mass. Fracture characteristics obtained from mapping and core, along with the hydraulic conductivities were used in a continuum fracture flow model. This model predicted flow in a westerly direction. Coupled with a conceptual model of the major structural and mining features of the area, it was determined that fluid flow away from the stope would continue in a northwesterly direction for approximately 610 m to a tunnel designed to drain local area mines. The nature of the fractures would most likely cause any tracer in the fluids originating at the stope to disperse to undetectable levels within a distance of travel of about 670 m (Miller, 1993).

### TRACER TESTS

A Class 5, Safe Drinking Water Act, Underground Injection Control Program rule authorization was obtained from the Environmental Protection Agency (EPA), to inject NaCl and water into the prototype stope. Under the rule authorization, injected concentrations were not to exceed 7,000 ppm NaCl (equivalent to 12,600  $\mu$ S/cm) solution.

To detect escaping tracer solutions from the stope, the stope and boreholes surrounding the stope were equipped with conductivity/temperature probes. Some of

the boreholes and the stope were equipped with pressure transducers to obtain water level data. A programmable data logger recorded the changes in conductivity and water levels at the site.

A series of tracer tests was conducted under a natural, but varying gradient to simulate and evaluate ground water flow directions that might be present during actual leaching conditions. The stope was filled with tracer and allowed to drain, similar to flood leaching. A variable hydraulic gradient was caused by the falling head in the stope during the tests, which made Darcy's Law difficult to apply. Conductivity data obtained from the tests were used to determine tracer transport velocities through the rock mass, relative dispersion of the tracer, and location of fractures and fractured areas that conducted the tracer away from the stope, keeping the variable gradient in mind. A center of mass of the tracer path could not be determined prior to monitoring borehole installation; therefore, it was not known if the center of mass would pass near the monitoring locations.

Three tracer tests were conducted over a period of 15 months in three steps or levels (figure 5). Each level exposed new fractures to the tracer solutions, and each test exposed fractures to a higher concentration of NaCl (figure 5). In the first tracer test (test 1), a total of 15,132 L of 3,000  $\mu\text{S}/\text{cm}$  solution of NaCl mixed with water was injected over a period of about an hour into the stope to a depth of 2.65 m (figures 6 and 7). During the test, the concentration of the salt in the stope declined as the water level declined. This conductivity decline could have been due to some dilution either from natural ground water existing in fractures adjacent to the stope or water flow into the stope.

Several days after the stope was filled, a drip developed in fractures directly above the stope in the roof of the upper chamber. This drip could have developed due to capillary flow through very small, continuous fractures from the bottom of the stope to above the stope. The dripping fluid was found to have high concentrations of the chloride ion; therefore, this fluid was the injected tracer because the chloride ion was not found in the background water. After 2 to 3 days the dripping ceased, but a damp fracture surface above the stope has remained to date. The dripping resumed during the second test (test 2), but was not observed during the third test (Test 3), nor during the constant head test.

A new set of fractures located higher in the stope was introduced to 22,702 L of the tracer solution in test 2. The concentration of the injected tracer in this test was measured to be 3,700  $\mu\text{S}/\text{cm}$ . Because 7,570 additional liters of tracer were added to the stope in test 2, a greater pressure head was applied to the fractures exposed to the tracer, than during test 1. Therefore, fluid could be forced in to smaller, tighter fractures where the fluid could not do so in the first test. It is believed that the conditions, mentioned above, which are required for capillary flow to exist, had changed by the time the third test was conducted.

The top third of the fractures in the stope were exposed to the tracer solutions in test 3. A total of 30,711 L of tracer with a concentration of 9,000  $\mu\text{S}/\text{cm}$  was injected into the stope during this test.

After each test, the fractures were flushed at least once with fresh water. The purpose of flushing the fractures was to dilute the salt solution within the fractures and to lower the background salt concentrations for the following test(s). These flushes were conducted in the same manner as the tracer tests by injecting water into the stope. Data were collected for each flush. The last flush test was conducted over a period of several weeks. The purpose of this last test was to maintain a constant head of water within the stope in order to collect additional data not provided during the previous "falling-head tests." Results of this "constant-head test" are also included in this report.

The amount of solution involved in the three tracer tests, subsequent stope flushes and the constant-head test totaled 476,522 L with 68,545 L of which was NaCl tracer solution, 312,246 L was fresh water in the constant-head test, and 95,731 L was fresh water in the stope flushed between tracer tests. The tracer test portion of the research covered a period of 15 months with varying levels of activity. Approximately 20 percent of the total tracer solution was captured at the bulkhead seepage trench and disposed of according to the EPA Class V Injection Well Rule Authorization.

#### Tracer Observations

Tracer was observed in four boreholes, numbers 3, 4, 6, and 7, during the course of the three tracer tests. The tracer was never detected in boreholes 5, 8, 9, 10, 11, and 12 during these tests. Explanations as to why the tracer never appeared in the boreholes include the possibility that: these boreholes may have not been hydraulically connected by fractures, or a falling head in the stope did not give the fluids a chance to be driven toward the boreholes.

The first arrival times and peak conductivities near these first arrival times were used to estimate flow velocities rather than the longer times-to-peak in each of the detection boreholes.<sup>10</sup> This is because the tracer conductivities did not readily decrease with time within the boreholes, probably due to stagnant tracer left behind in the borehole as the falling level of tracer in the stope dropped below the connecting fractures.

---

<sup>10</sup>Kunkel, J., CO. Sch. of Mines, Private Communication Nov. 1, 1994.

## Borehole 6

Borehole 6 was one of the two locations in the path of the tracer during the first tracer test. Tracer monitoring data also showed this borehole was coincidentally in close proximity to the center of mass of the travel path of the tracer. This was the only outlying location where the tracer was detected in the first test (figure 2). The direction of flow toward this borehole (west to northwest) coincides with predictions made by modeling flow in which a constant gradient was assumed at the site using fracture data (Miller, 1993).

The first arrival of the tracer in borehole 6 was at 1,186 minutes (19.8 hrs), and the peak conductivity of 2,900  $\mu\text{S}/\text{cm}$  was detected at 3,758 minutes (2.6 days) (figure 8 and table 1). The concentration after the first arrival of tracer gradually rose in steps, but after a while the concentration dramatically increased to higher levels. This first arrival is probably due to saturated fractures carrying the tracer relatively quickly toward the borehole. The tracer concentration was also diluted with existing water in these fractures, therefore a small rise in concentration is observed. The higher concentration jumps following the first arrival of the tracer can be explained by slower movement and/or a longer path to the borehole along unsaturated to partially-saturated fractures. Hardly any dispersion or matrix diffusion of the tracer occurred since the injected concentration was 3,000  $\mu\text{S}/\text{cm}$ , therefore most of the flow toward the borehole was through unsaturated fractures. The number of fractures carrying fluid into the borehole is not known, but one assumption is that single fractures were responsible for each jump in concentration.

Borehole 6 is inclined, drilled at 32 degrees from horizontal (figure 2). Because of this, it is not known at which location along the borehole the tracer was intercepted. The borehole is located between 4.4 m and 10 m from the stope. The peak tracer travel velocity during the first test was calculated to be at least between  $1 \times 10^{-2} \text{ cm/s}$  and  $2 \times 10^{-2} \text{ cm/s}$ , assuming the tracer path was not tortuous and one fracture conducted the fluid to the borehole.

During the next two tests, the travel time of the first arrival tracer decreased to 240 minutes (4 hrs) for test 2 and 194 minutes (3.2 hrs) for test 3 (figures 9 and 10). The first arrival time was shorter in these next two tests because the fractures had been wetted by test 1. However, the travel time for the peak concentration increased in each test; 44,958 minutes (31.2 days) and 49,260 minutes (34.2 days), respectively (table 1). It would seem that the travel times for peak arrivals should have decreased in the consecutive tests; however, Tests 2 and 3 exposed new sets of fractures that allowed the tracer to leave the stope. Also the tracer had to travel through other fractures in the fracture system to reach the detection point and/or the pathway was initially unsaturated. Because more liters of tracer solution were added to the stope, this greater pressure head could have also forced the water through new pathways not used during test 1. In addition, the falling head in the stope could have had an effect



on the tracer movement through the new fractures. The combination of these factors is probably the reason for the slower peak travel times in both cases.

Figure 9 shows that flow was interrupted to borehole 6 during test 2. There are two possible explanations for this. The fracture(s) transporting the tracer to the borehole were blocked by fine particles flowing with the tracer or by swelling clay within the fracture. Later, the water pressure on the blockage jarred the particles or clay out of their positions, resuming flow to borehole 6. Blockage from entrapped air could have had a similar effect on the transport of tracer in the fracture network due to phase interference (Pruess and Tsang, 1990; Persoff and Pruess, 1995). A double peak was also present during test 3 (figure 10). This second peak is likely due to separate fractures transporting tracer. The fractures located on the sides of the stope, instead of those underneath the stope, are the ones responsible for transmitting the water away from the stope toward borehole 6, because the borehole was dry when 0.3 to 0.6 m of water remained in the stope.

### Borehole 7

Borehole 7 is located 3 to 5 m underneath the stope and parallel to the axis of the bottom drift (figure 2). Detected tracer concentrations instantly matched the injected concentration of 3,000  $\mu\text{S}/\text{cm}$  in this borehole during the first test. This instantaneous response in the borehole is probably due to a high degree of fracturing between the borehole and stope as a result of blast damage. Also, during test 1, the bulkhead began to leak, and the overflow went down borehole 7 for a couple hours until a pump and sump were installed to intercept this flow. Therefore, the data collected from this borehole after the overflow occurred were not accurate and were not used for analysis. Borehole 7 was abandoned for the next two tests, because it began to collapse.

### Borehole 3

During test 1, no changes in conductivity were observed in borehole 3. During the second test, however, a change in conductivity was recorded 36 minutes into the test (figure 11). This conductivity gradually increased until the test was stopped. The maximum conductivity was approximately 1/6 of the injected tracer concentration and was lower than concentrations seen in borehole 6. This borehole is vertical and is located approximately 1.2 m away from the stope. The tracer probably flowed directly from the stope to the borehole, because a response was seen only 6 minutes after the solution reached the test 2 concentration level in the stope where the new fractures were exposed. Test 3 suggests a new tracer path was taken or air blockage occurred because the first arrival time was longer than in test 2 (figure 12). In this test it took 149 minutes (2.5 hrs) for the first arrival of tracer to be detected. However, the maximum tracer concentration was reached in one-half the time than that from test 2. The tracer may have been cut off from finding other new paths in the rock mass, because the water level in the stope started dropping quickly. The maximum

concentration in the last test was approximately 1/8 of the injected tracer concentration. Water levels were recorded in this borehole during the third test. The water level was fairly constant for the first week of the test, but began to steadily decline soon after because of the declining head in the stope.

Tracer transport velocities for the first arrival of tracer were calculated for each test. The velocity for the second test was found to be  $5.6 \times 10^{-2}$  cm/s, and the velocity in the third test was found to be  $1.3 \times 10^{-2}$  cm/s assuming transport occurred within only one fracture.

#### Borehole 4

Tracer was detected in borehole 4 only during test 3. Flow still continued toward boreholes 6 and 3, but this new set of fractures seemed to quickly conduct the tracer toward borehole 4. The top third of the rock mass between borehole 4 and the stope was found to be very densely fractured when drilling borehole 4. This fracturing probably contributed to the quick response in tracer detection in this borehole. Water was lost during drilling, and hydraulic conductivities averaged about  $3.9 \times 10^{-3}$  cm/s in this borehole during the water packer tests (Miller, 1993). These hydraulic conductivities were obtained between the depths of 2.4 and 4.2 m in this borehole. Because the head started dropping in the stope rapidly after injection (figure 13), this connection between the stope and borehole 4 was soon discontinued. During the test, water could be observed running out of these fractures into the borehole. Tracer transport velocity was calculated to be  $2.3 \times 10^{-2}$  cm/s. The first arrival of the tracer was observed after 102 minutes (1.7 hrs), but this was about the same time that the water level was reached in the stope that hydraulically connected the fractures between the stope and borehole; therefore, the transport velocity was calculated from the time the water level in the stope reached the connecting fractures.

A second peak of tracer was observed at 92,469 minutes (64.2 days) into the test (figure 14). This peak could have been caused by the tracer taking several different paths to the detection point.

A "reverse test," in which borehole 4 was filled with water, was conducted when the stope was drained after test 3. This was done to note location of the direct communication between the borehole and the stope. When borehole 4 was filled, the stope showed a draining fracture located approximately 1 m from the base of the stope. This fracture was connected to a fracture located near the top of borehole 4. Thus, this system of fractures was hydraulically connected.

#### Constant-Head Test

Previous tracer tests were conducted by filling the experimental stope to different elevations with each test subjecting fractures at higher elevations to tracer solution.

The solution flow for these tests was stopped when the predetermined elevation was reached in the stope for each test. Data were collected at boreholes surrounding the experimental stope as the solution level in the stope decreased. The solution level in the stope for the third tracer test (test 3) was within 0.46 m from the stope top (depth of 7.77 m). Upon completion of the three tracer tests and their subsequent falling-head flush with fresh water, a constant-head test using fresh water was conducted.

The constant-head test was initiated by filling the experimental stope with fresh water to within 0.46 m from the top. The elevation of the water was maintained by use of a float valve that activated the inflow pump on the level below when the water level in the stope dropped approximately 5 cm. The float valve was attached by an adjustable rod to an electrical switch mounted in a box on the grating that covers the stope. As the water level dropped, the float would descend, pulling the rod until the switch was activated. As the water level then rose, the float would push the rod until the switch was deactivated.

As in the previous tracer tests, electronic data collection was conducted in the boreholes surrounding the experimental stope using a multichannel data logger to which various probes were attached by cable. The probes were placed at the bottoms of the surrounding boreholes and measured the conductivity or pressure. Analysis of these data is discussed in detail later in this section.

Manual data, involving incremental flowmeter readings and elapsed time, were collected during periodic inspections of the experimental leaching stope while the constant-head test was being conducted. Three periods of data collection occurred because there were two interruptions to constant-head testing. These interruptions caused the water level in the stope to fluctuate (figure 15). Despite complicating the interpretation of data, these fluctuations were used to give additional information on the degree of saturation of the site and connectivity of various boreholes with the stope. By comparing water level data during the fluctuations and draining of the stope after the constant head test and test 3, it was found that the stope area was becoming slightly more saturated with time as more water was being introduced to the fractures. Figure 22 shows the rate at which fluid levels within the stope decreased over time during the constant-head test and test 3. A power surge disabled the return pump, which caused the first test interruption. The total solution inflow to the stope was obtained, but no valid incremental flow data were collected. The second interruption resulted from a pipe connection failure. This failure occurred while researchers were present, which allowed validation of incremental flow data, as well as total flow verification. The third period was uninterrupted.

The solution flow into to the rock mass was calculated as the difference between the total solution inflow to the stope less the solution outflow around the bulkhead. Manual readings were available from the second and third constant-head test periods. During the second period, the total solution flow rate into the experimental stope

averaged 13.78 L/min over an approximate 8-day interval. Incremental solution flow, averaging 13.97 L/min, was measured during the third day of the second period. This compares closely with the total flow rate of 13.78 L/min. Solution loss from the stope due to bulkhead seepage averaged 1.25 L/min during the second period of constant-head testing. The remaining solution in the stope flowed into the rock mass at a rate of 12.53 L/min. Incremental solution loss, averaging 13.06 L/min, was measured after the test had been in progress for 24 hours. This compares closely with the total loss rate of 13.06 L/min. Solution loss from the stope due to bulkhead seepage averaged 1.21 L/min during the third period of the constant-head testing. The remaining 11.74 L/min flowed into the rock mass surrounding the stope.

The total flow rate from the experimental stope into the rock mass under constant-head conditions decreased from an average of 13.78 L/min to 12.95 L/min; a decrease of 6 percent which was confirmed by the incremental total loss rate. The loss rate through the bulkhead decreased approximately 3 percent (1.25 versus 1.21 L/min) with a resulting calculated loss rate decrease to the rock mass of 6.3 percent (12.53 versus 11.74 L/min).

Idaho Springs city drinking water was injected into the stope without a tracer for test 3. During injection, the water in the stope reached a maximum conductivity of 400  $\mu\text{S}/\text{cm}$ . During the time a constant head was being maintained in the stope, the conductivity inside the stope began to rise before dropping off again. This gradual rise in conductivity was due to the salt solution from the previous tracer tests traveling back toward the stope along the true hydraulic gradient. During the previous tracer tests and the beginning of the constant head test, the rock mass was relatively unsaturated in comparison to later on in the constant head test. At the time of injection the hydraulic gradient was very steep in all directions, since a driving head of fluid was being introduced. As the water level in the stope was maintained, the hydrologic conditions around the stope approached steady state, thus fluid movement within the fracture networks approached its true hydraulic conductivity and gradient.

The constant-head test showed that a large amount of tracer remained within the fractured rock mass around the stope after the tracer tests were completed. Since the driving force (water head in the stope) was removed after each tracer test, the tracer was either stagnant in the fracture network or very slow moving. During the third period of constant-head testing, the total solution injection rate into the experimental stope averaged 12.95 L/min over an approximate 3-day interval. Conductivities measured in most of the boreholes surrounding the stope were also considerably higher than the conductivity measured in the stope as the residual tracer from the previous tests was transported ahead of the water toward these boreholes.

### Borehole 3

Conductivity in borehole 3 steadily increased over the course of the constant-head

test (figure 17). The conductivity measured in the borehole during this test was two to four times higher than the measured conductivity in the stope. Data were collected at borehole 3 for only 8,700 min (6 days) due to a defect in the probe; it is not known, therefore, how long the conductivity in the borehole would have continued to increase. Measurements made in this borehole did not seem to be affected by the fluctuation in water level in the stope during testing. Using the water as the tracer, a travel velocity was calculated to be  $1.1 \times 10^{-2}$  cm/s, which is slower than during the previous tracer tests, assuming transport was through the same set of fractures.

#### Borehole 4

Conductivity data collected in borehole 4 were found to be quite erratic during the constant-head test. Although conductivity in the borehole did not seem to be affected by the fluctuations of water level in the stope, draining the stope had a large impact on the conductivity (figure 18).

Sharp increases in conductivity were observed in this borehole at about 8,720 min (6 days) and at 20,580 min (14.3 days), as well as a sharp decrease in conductivity at 22,040 min (15.3 days). These changes may be due to the effect of residual tracer transport by certain fracture families or sets.

#### Borehole 6

The conductivity in borehole 6 quickly increased to 3,100  $\mu$ S/cm in 1,380 min (23 hrs) (figure 19). After reaching this maximum concentration, the concentration decreased in three sharp drops. Data collected in this borehole did not seem to be affected by changes in water level in the stope.

#### Borehole 8

During test 1, only water level data were collected in this borehole. Data showed that tracer migrated to the borehole, but only amounted to several centimeters of head. During tests 2 and 3, conductivity data were collected in borehole 8; however, no significant changes occurred in the borehole during these two tests. Observed conductivities in borehole 8 during the constant-head test were the most erratic (figure 20). These data did not seem to correlate with any observations from previous tests or stope level data.

#### Borehole 10

Although this borehole never showed a response to tracer in the previous tests, the constant-head test showed that a connection between the stope and borehole did exist. Figure 21 shows the observed tracer concentrations in borehole 10 during the last test. Concentration rose slightly in the borehole after 4,000 min (2.8 days) and fluctuated

for another 4,500 min (3.1 days). It cannot be determined whether these early data were affected by the change in water level in the stope. At 8,700 min (6 days) the conductivity abruptly rose to 1,200  $\mu\text{S}/\text{cm}$ . It is unlikely that this change was related to the same fracture system(s) as the earlier data. This later data maintained a constant concentration until the end of the test.

By keeping a constant head in the stope, more fractures were allowed to conduct fluid. Borehole 10 showed direct evidence of this, since this borehole remained dry in the first three tracer tests and showed a response in the constant-head test.

Data collected in borehole 6 showed the expected response for the constant head test--a peak in conductivity, then a decline in conductivity. This decrease in conductivity was not gradual, indicating that not much mixing was occurring within some of the fractures. However, the other boreholes showed hardly any decrease in conductivity. Either data collection ceased before this decrease could be observed, blockage could have occurred within fractures as it did during the tracer tests, or no mixing occurred within the fractures.

Stope-draining data from the constant-head test were compared to data from test 3, in which tracer was injected to the same level in the stope as in the constant-head test. These data show that the stope area became slightly more saturated with each test (figure 16).

## SUMMARY AND CONCLUSIONS

A simulation of leaching solution movement away from the experimental stope was conducted in which NaCl was used as a tracer. Observations were made and data was collected as to how fluid migrates within a fractured crystalline rock mass by detecting tracer in several borehole monitoring wells adjacent to the stope. The final test conducted at the experimental stope involved the injection of fresh water, without the NaCl tracer, which was kept at a constant head for several weeks.

Water from the final test chased the tracer through various fracture networks. Observations concerning fluid migration during this constant head test were compared to the data collected during the previous tracer tests under a falling head pressure.

The following data results are summarized concerning solution control at this site:

- Geologic characterization of the site was an important factor in interpreting of the tracer test results and modeling fracture flow (Miller, 1993).
- The degree of fracture connectivity, rather than fracture density, is instrumental in conducting fluids. This is consistent with other research conducted on the influence of fracture geometry on fluid transport (Snow, 1969; Long, 1985; Smith and Schwartz, 1984).

- Solutions can migrate by capillary flow through continuous small aperture fractures and a constant supply of fluid.
- Saturated and unsaturated fractures conduct solution in different ways (refer to tracer test section on borehole 6). This was observed as the stope area became more saturated with the progression of each test (figure 16).
- Conducting the tests at varying depths of tracer solution within the stope effectively isolated certain fractures, similar to the use of packers in boreholes/wells.
- As the pressure head inside the stope increased, the tracer found new pathways through tighter, smaller fractures (refer to borehole 10 during the constant-head test).
- Without nearby water pressure, fluids within the fractures became stagnant or flowed very slowly.
- While maintaining a constant head with fresh water, the tracer conductivity inside the stope increased, indicating steady-state conditions were being reached with respect to the hydraulic gradient.

Data obtained from manual and electronic readings indicated that the following procedures can be useful in designing for solution control in stope leaching:

- Grouting is one technique to prevent solutions from taking certain pathways. Grouting would decrease the permeability of the rock mass and fracture connectivity. Surface grouting in the test stope area reduced leakage, where applied, by a factor of 100. Rock mass characterization to locate probable geologic solution conduits combined with pressure grouting can significantly reduce fluid flow through areas inaccessible to surface grouting.
- Pumping solution from a borehole or using interception wells could be an alternative for solution control. A leachant could be pumped out of such boreholes and processed or recycled for reuse, thus developing a remediation-leaching cycle. Pumping in combination with grouting could be considered as solution control with a safety factor.
- Blasting techniques to minimize wall rock damage were useful in minimizing the need for solution control external to the leaching stope. Tracer was quickly observed in boreholes 3, 4 and 7 where the rock was more susceptible to blast damage.
- Data from the constant head test showed a measurable reduction in solution loss within days as the hydrologic conditions in the rock mass surrounding the stope approached steady state. Pre-injection of an innocuous fluid into a stope until steady state is reached, would identify fractures or areas of fluid loss for solution control.

#### ACKNOWLEDGMENTS

The authors wish to thank Mr. Bill Strickland, Mine Manager of the Edgar Mine, Stope Leaching team members, and Dr. James Kunkel, adjunct professor at the Colorado School of Mines Geology Department, for their help and suggestions in the solution control phase of the project.

## REFERENCES

- Boreck, D. L., and J. M. Goris. Reduction of Surface Mineral Waste Through Underground In Situ Leaching of Fragmented Ore and Fill Material. Paper in Proceedings of Second International Conference on Environmental Issues and Management of Waste in Energy and Mineral Production, (Calgary, Alberta, Canada, Sept. 1992), Balkema/Rotterdam, 1992, pp. 951-959.
- Florquist, B. A. Techniques for Locating Water Wells in Fractured Crystalline Rocks. *Ground Water*, v. 11, No. 3, 1973, pp. 26-28.
- Harrison, J. E., and R. H. Moench. Joints in Precambrian Rocks, Central City - Idaho Springs Area, Colorado. U.S. Geol. Surv. Prof. Paper 374-B, 1961, 14 pp.
- Hutchinson, R. M. Geological and Structural Setting of the CSM/OCRD Test Site: CSM Experimental Mine, Idaho Springs, Colorado. Technical Report, CO. Sch. of Mines, Golden, CO., Sept., 1983, 47 pp.
- In-Situ Inc. Software and Plume User's Guide. V2.1, Computer Technology Division, Laramie, WY, Dec. 1986, 44 pp.
- INTERA Environmental Consultants, Inc. Porosity, Permeability, and Their Relationship in Granite, Basalt, and Tuff. Technical Report, Apr. 1983, ONWI-458, Houston, TX, 63 pp.
- Jessop, J. A., D. L. Boreck, M. J. Jackson, and D. R. Tweeton. Evaluation of a Stope Leaching Site Using Geotomography. Paper in Proceedings of In-Situ Minerals Recovery II, Engineering Foundation, NY, 1994, pp. 599-616.
- Long, J. C. S. Verification and Characterization of Continuum Behavior of Fractured Rock at AECL Underground Research Laboratory. Lawrence Berkeley Laboratory, Univ. of California, BMI/OCRD-17, 1985, 239 pp.
- Lutzens, W. W. Rock Mass Characterization for In-Stope Leach Solution Containment. Paper in Proceedings of In-Situ Minerals Recovery II, Engineering Foundation, NY, 1994, pp. 381-404.
- Miller, N. C. Predicting Flow Characteristics of a Lixiviant in a Fractured Crystalline Rock Mass. USBM RI 9457, 1993, 24 pp.
- Moench, R. H., and A. A. Drake. Economic Geology of the Idaho Springs District, Clear Creek and Gilpin Counties, Colorado. U.S. Geol. Surv. Bull. 1208, 1966, 91 pp.



Persoff, P. and K. Pruess. Two Phase Flow Visualization and Relative Permeability Measurement in Natural Rough-Walled Rock Fractures. *Water Resources Research*, Vol. 31, No. 5, 1995, pp. 1175-1186.

Pruess, K. and Y. W. Tsang. On Two-Phase Relative Permeability and Capillary Pressure of Rough-Walled Rock Fractures. *Water Resources Research*, Vol. 26, No. 9, 1990, pp. 1915-1926.

Smith, L. and F. W. Schwartz. An Analysis of the Influence of Fracture Geometry on Mass Transport in Fractured Media. *Water Resources Research*, Vol. 20, No. 9, 1984, pp. 1241-1252.

Snow, D. T. The Frequency and Apertures of Fractures in Rock. *J. Rock Mech. Min. Sci.*, Vol. 7, No. 1, 1970, pp. 23-40.

Snow, D. T. Anisotropic Permeability of Fractured Media. *Water Resources Research*, Vol. 5, No. 6, Dec. 1969, pp. 1273-1289.

Snow, D. T. Fracture Deformation and Changes of Permeability and Storage Upon Changes of Fluid Pressure. *Quarterly of the CO. Sch. of Mines*, v. 63, No. 1, 1968a, pp. 201-244.

Snow, D. T. Rock Fracture Spacings, Openings, and Porosities. *J. of the Soil Mechanics and Foundations Division, Proceedings of the American Society of Civil Engineers*, Jan. 1968b, v. 94, No. SM1, 1968b, pp. 99-117.

Table 1.—Tracer test results

Test	Start date	Baseline conductivity, $\mu\text{S}/\text{cm}$	Initial NaCl conductivity, $\mu\text{S}/\text{cm}^1$	Injection zone, m	First arrival		Peak arrival		Tracer velocity, $\text{cm}/\text{s}$
					time, min	conductivity, $\mu\text{S}/\text{cm}$	time, min	conductivity, $\mu\text{S}/\text{cm}$	
WELL 3, 1.2 m FROM STOPE									
2 . . . . .	11/10/93	300	3,700	0-6.0	36	300	83,898	<sup>2</sup> 550	0.056
3 . . . . .	05/13/94	650	9,000	0-8.8	149	650	46,680	<sup>2</sup> 1,100	0.013
CH . . . . .	09/14/94	800	400	0-8.8	175	800	8,240	<sup>2</sup> 900	0.011
WELL 4, 1.4 m FROM STOPE									
3 . . . . .	05/13/94	0	9,000	0-6.0	120	9,200	1,324	9,500	0.023
CH . . . . .	09/14/94	3	400	0-8.8	135	700	21,850	1,100	0.017
WELL 6, 10 m FROM STOPE									
1 . . . . .	06/25/93	0	3,000	0-2.7	1,186	60	3,758	<sup>2</sup> 2,900	0.014
2 . . . . .	11/10/93	2,000	3,700	0-6.0	240	2,000	44,958	3,100	0.069
3 . . . . .	05/13/94	2	9,000	0-8.8	194	100	49,260	7,900	0.086
CH . . . . .	09/14/94	700	400	0-8.8	560	200	3,540	3,100	0.030
WELL 8, 10 m FROM STOPE									
CH . . . . .	09/14/94	30	400	0-8.8	115	350	20,340	650	0.115
WELL 10, 3+ m FROM STOPE									
CH . . . . .	09/14/94	3	400	0-8.8	4,260	100	8,820	1,200	>0.001

CH Constant head.

<sup>1</sup>Conductivity of injected tracer in the stope.<sup>2</sup>Test ended before maximum conductivity was reached.

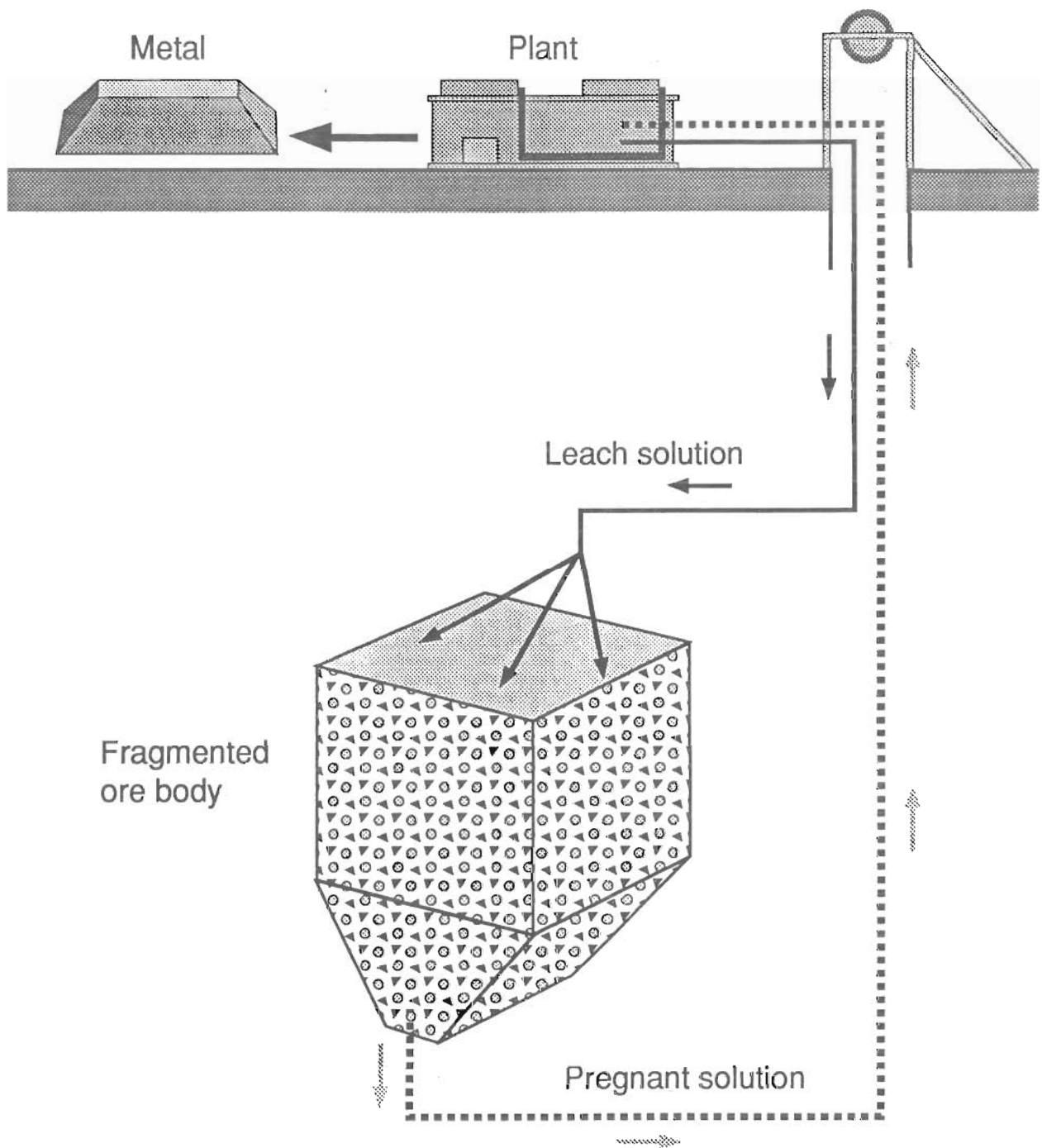


Figure 1. Schematic of stope leaching process in underground mines.

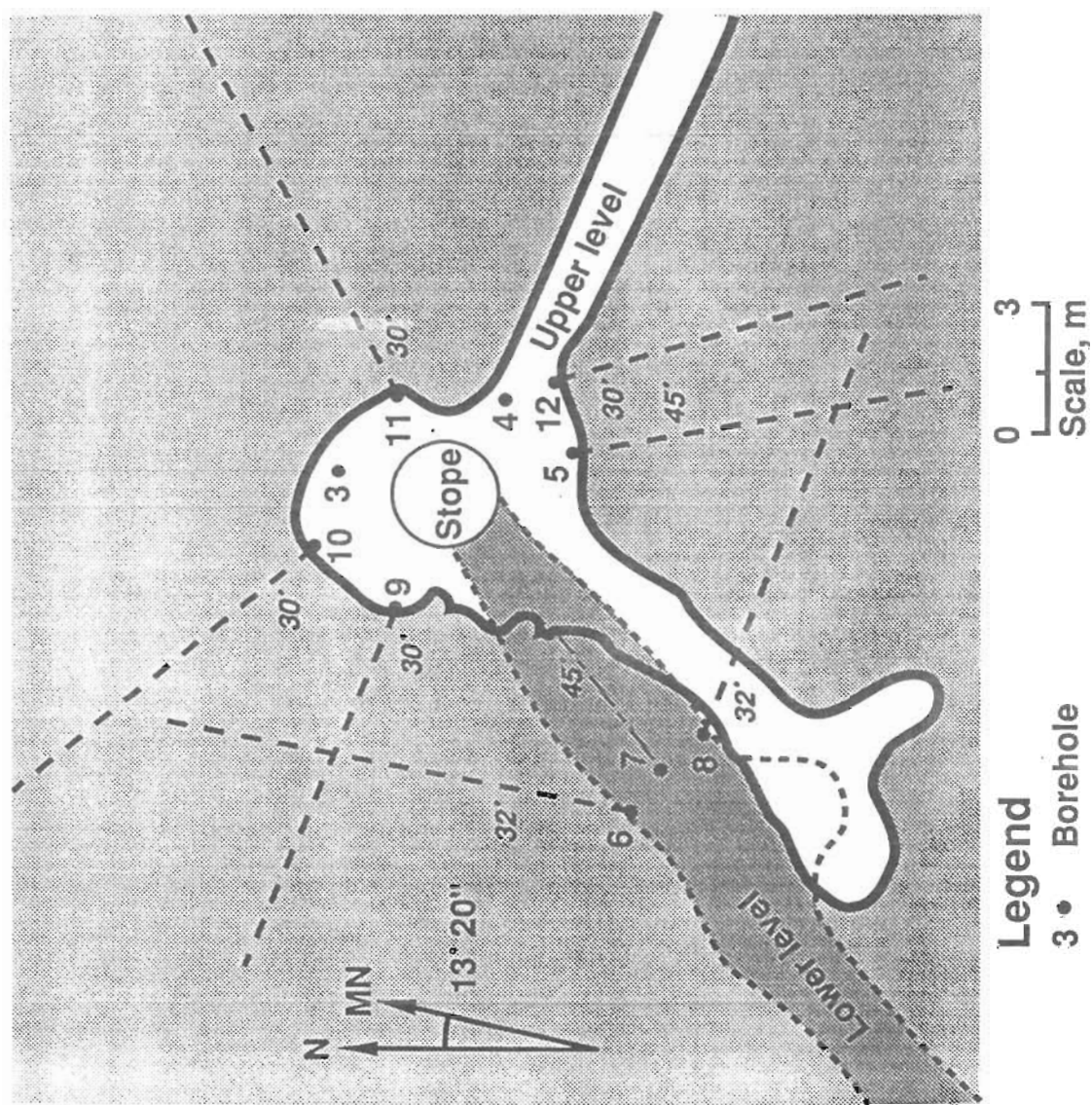


Figure 2. Plan view of the solution control research site showing borehole monitoring locations.

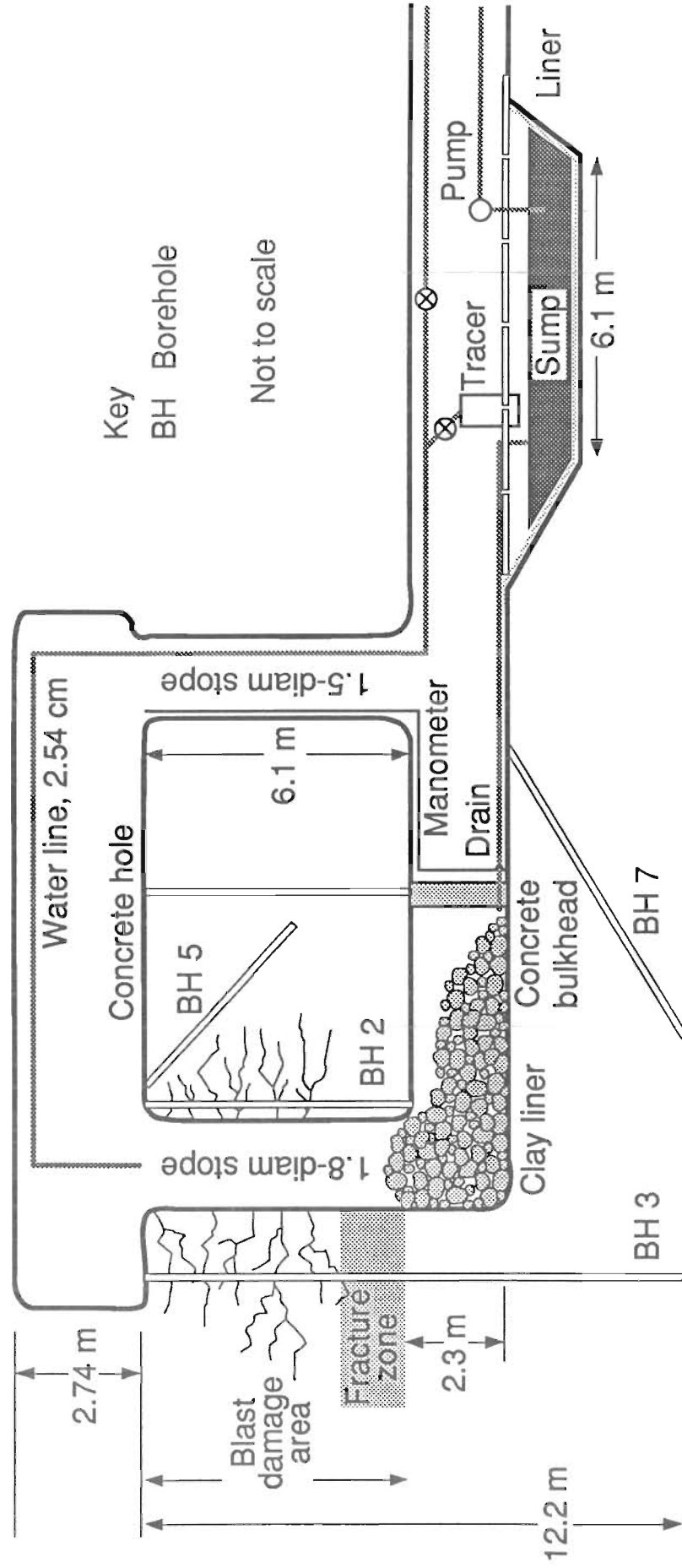


Figure 3. Longitudinal section of the stope and solution circulation system.

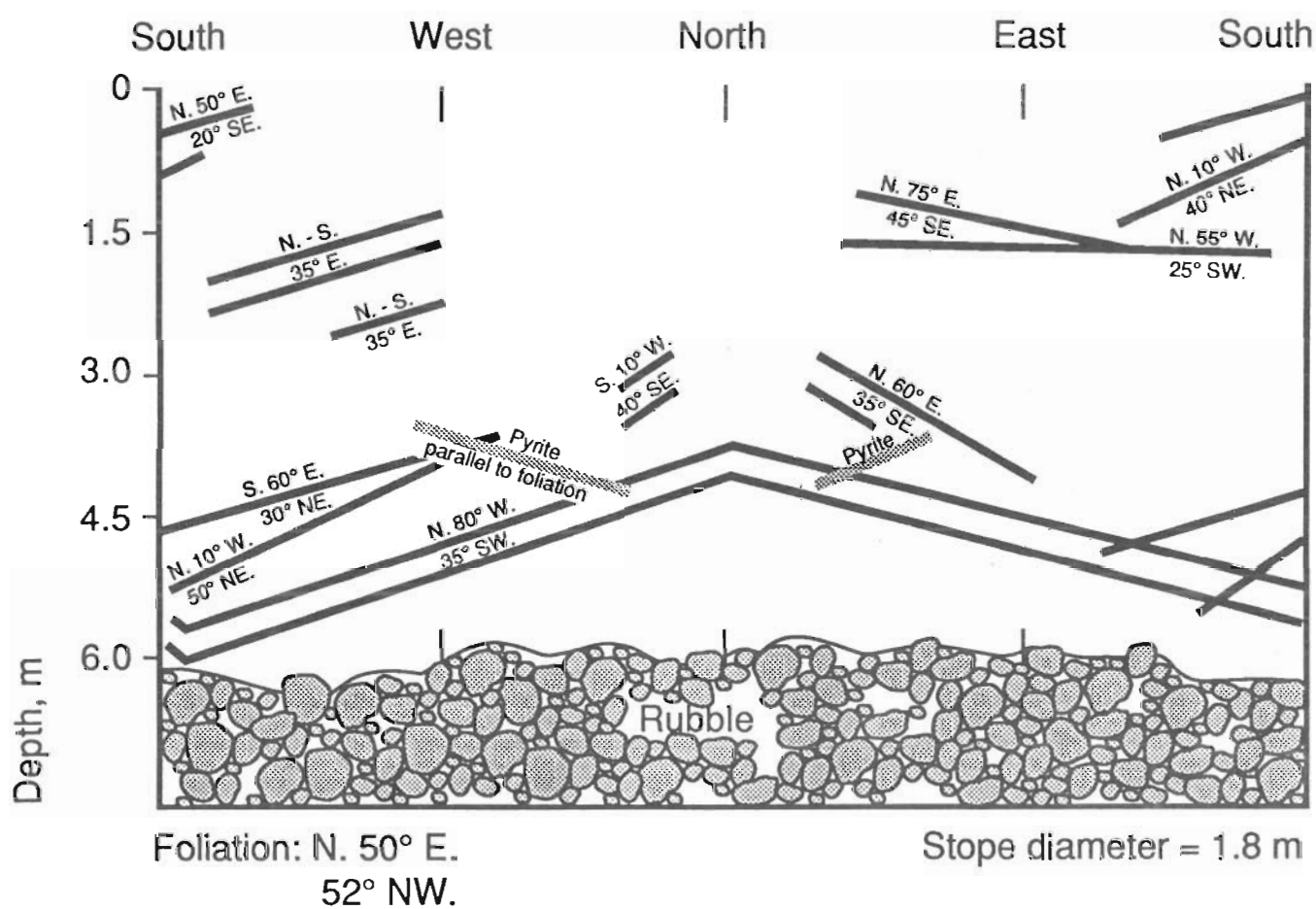


Figure 4. Orientation of fractures mapped inside the stope.

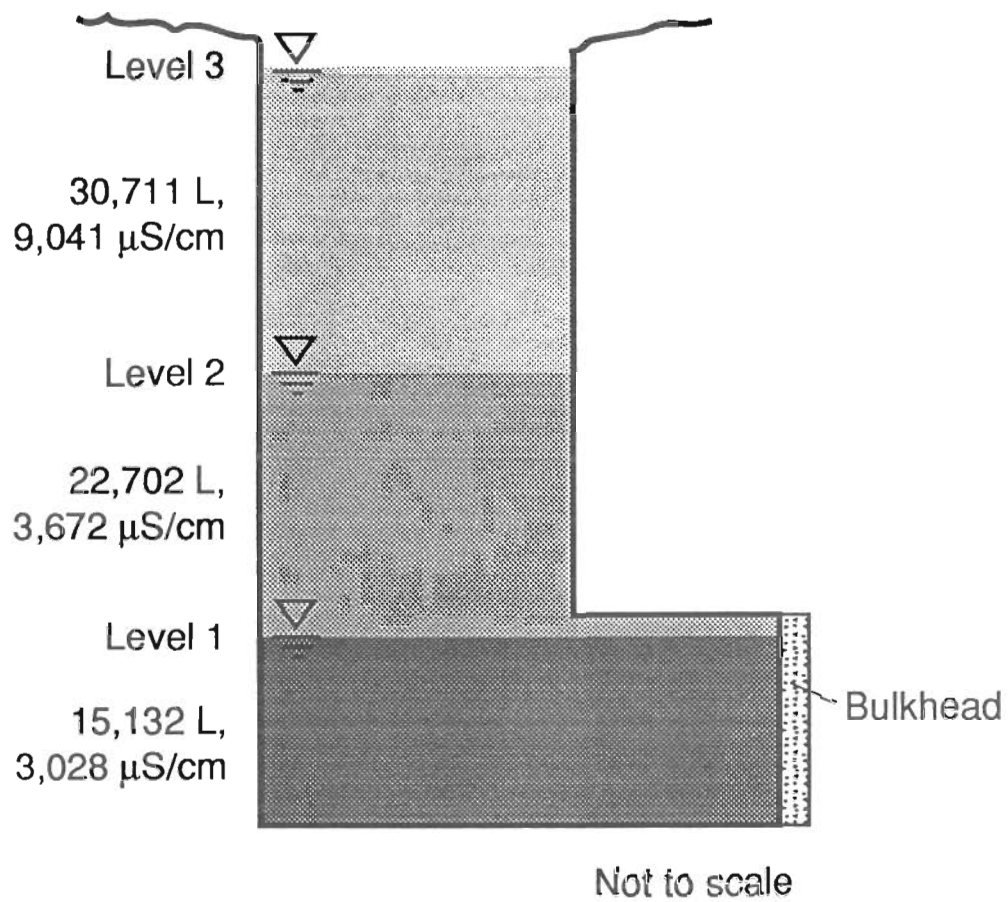


Figure 5. Tracer test levels and concentrations (Edgar test stope).

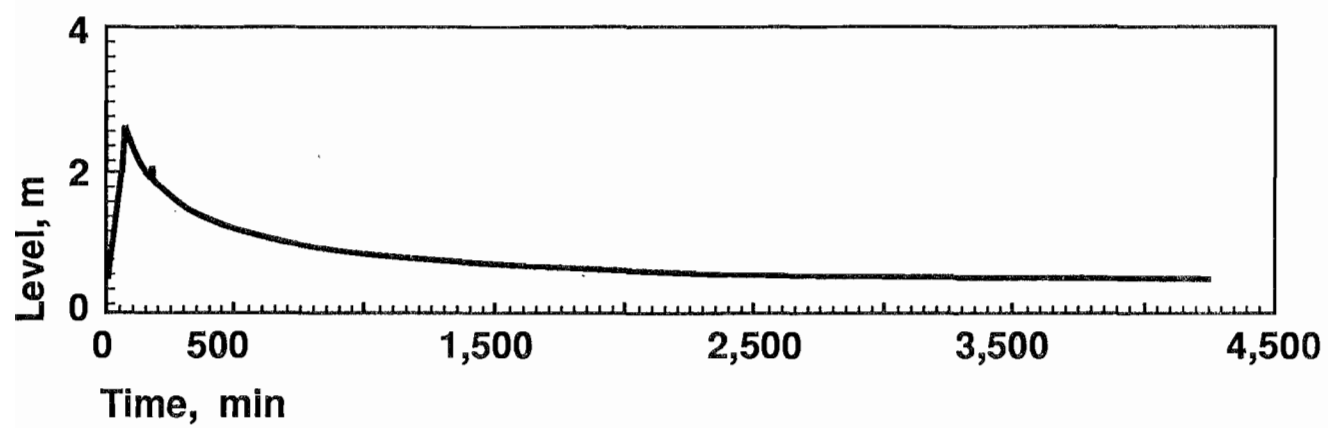


Figure 6. Tracer level in the stope during test 1.



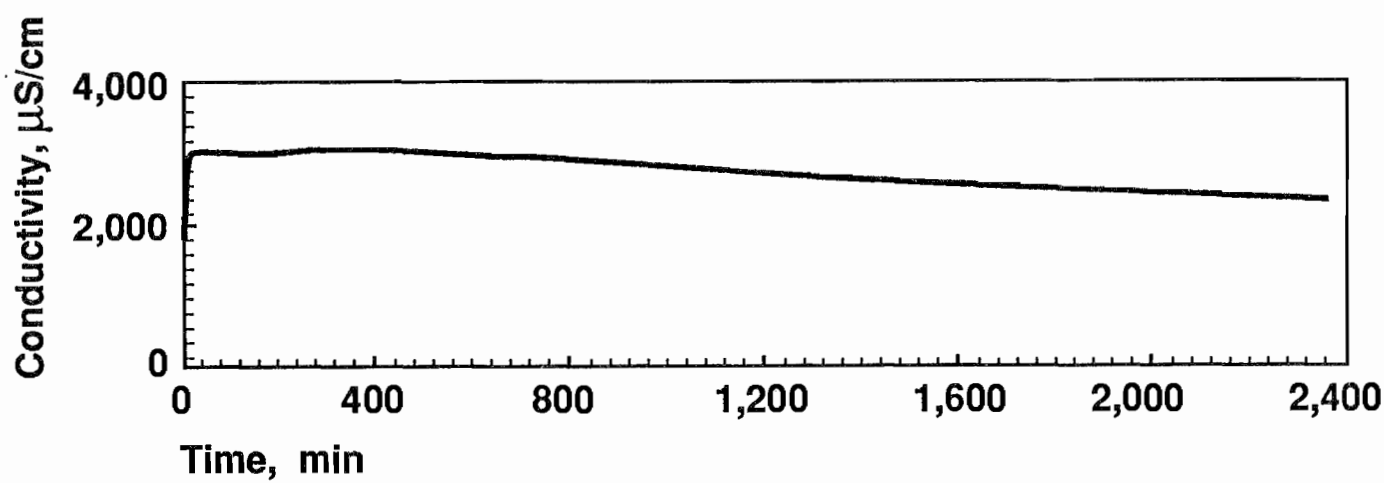


Figure 7. Conductivity in the stope during test 1.

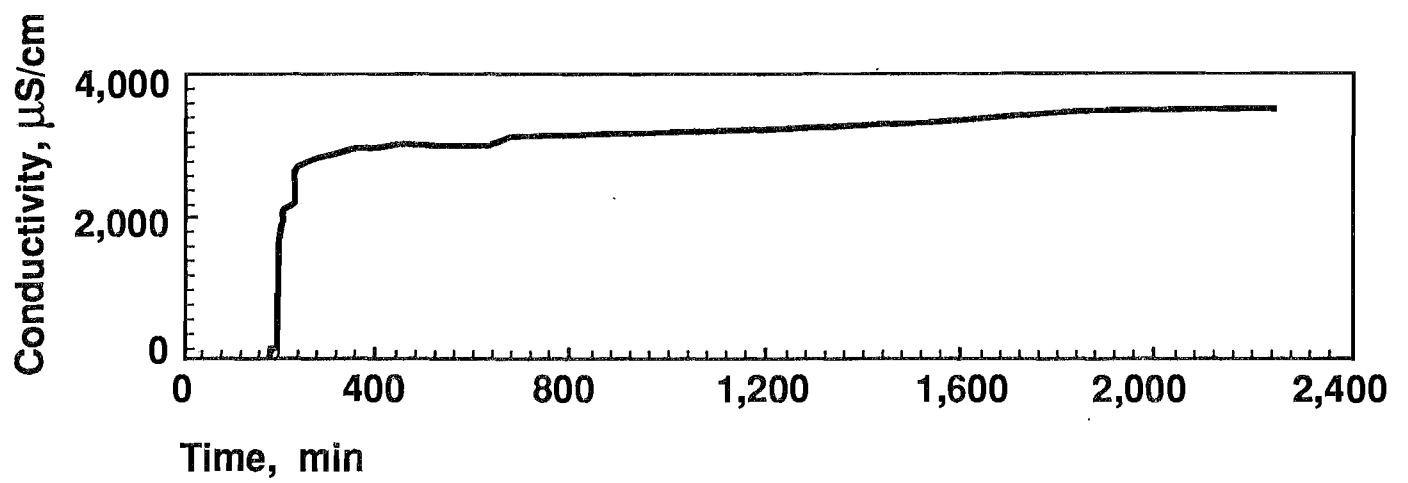


Figure 8. Borehole 6 conductivity during test 1.

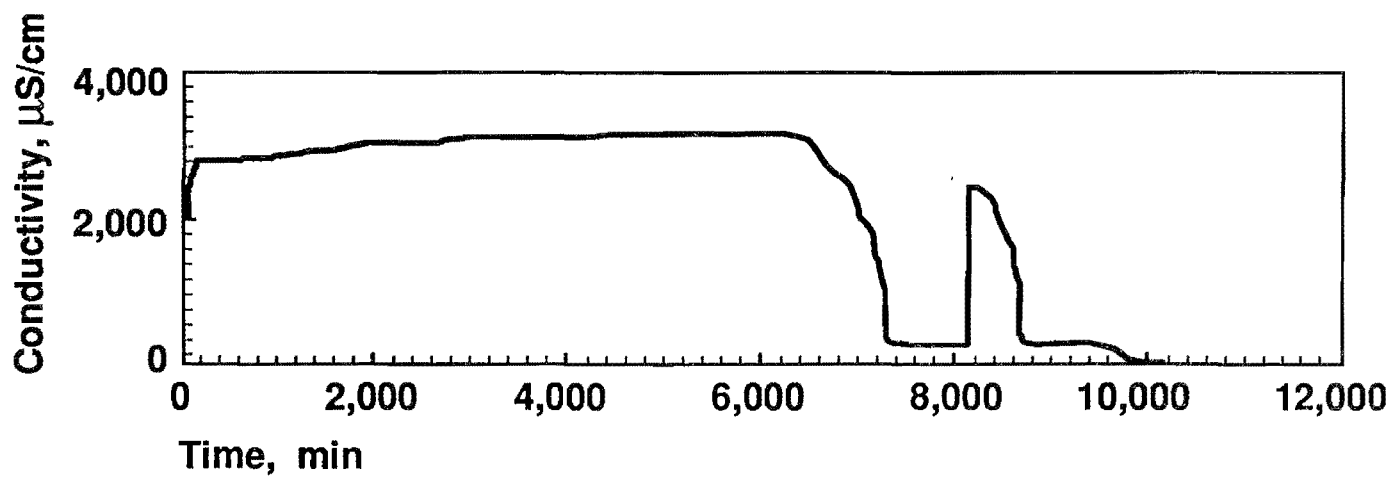


Figure 9. Borehole 6 conductivity during test 2.

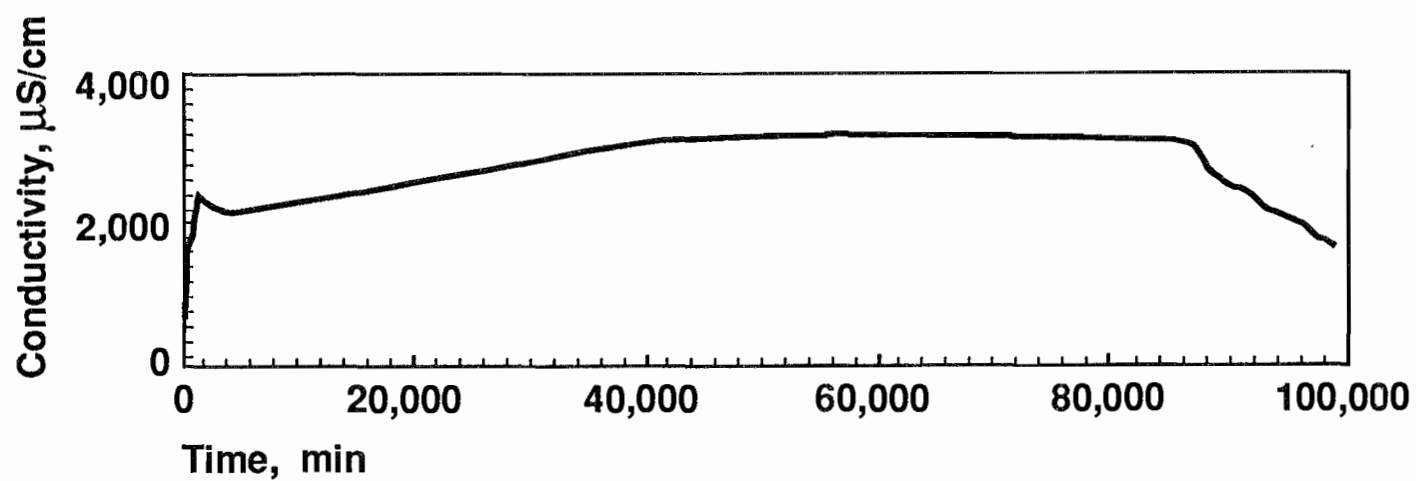


Figure 10. Borehole 6 conductivity during test 3.

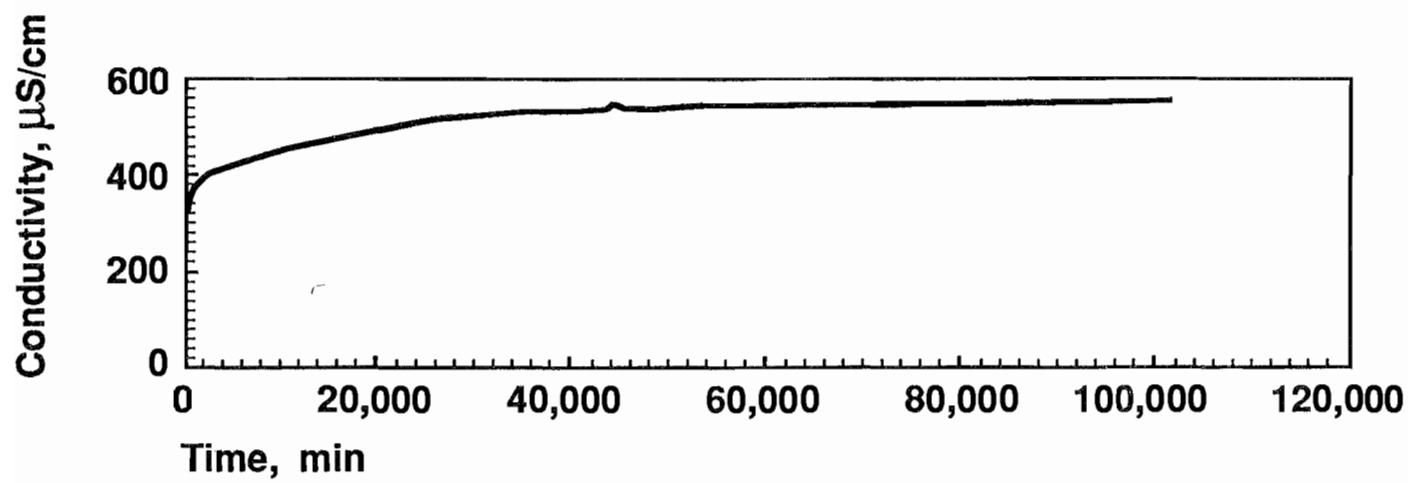


Figure 11. Borehole 3 conductivity during test 2.

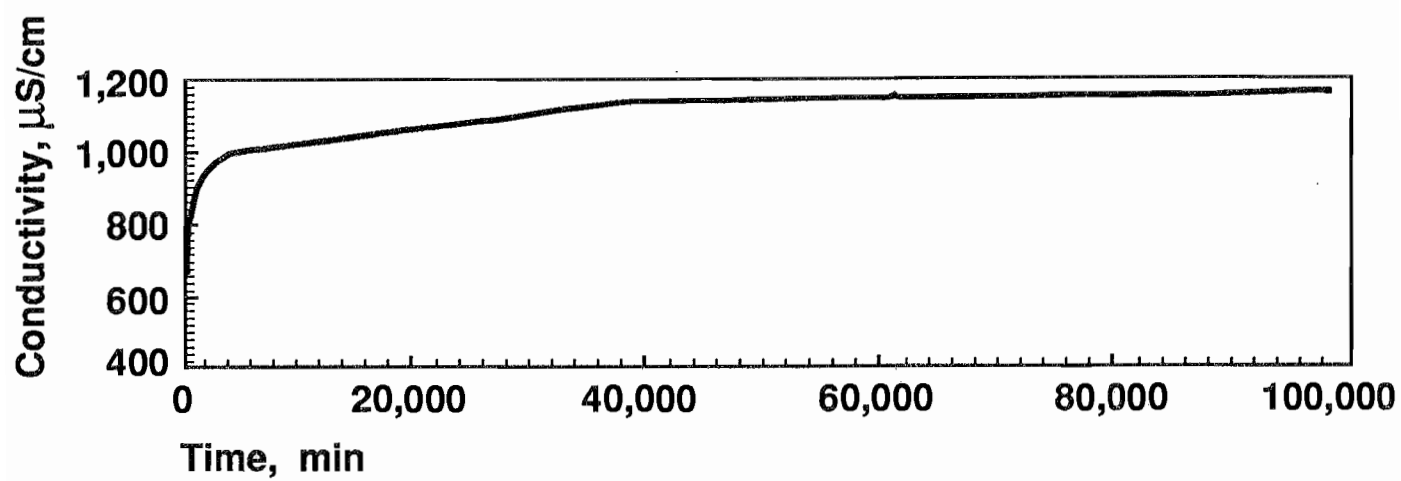


Figure 12. Borehole 3 conductivity during test 3.

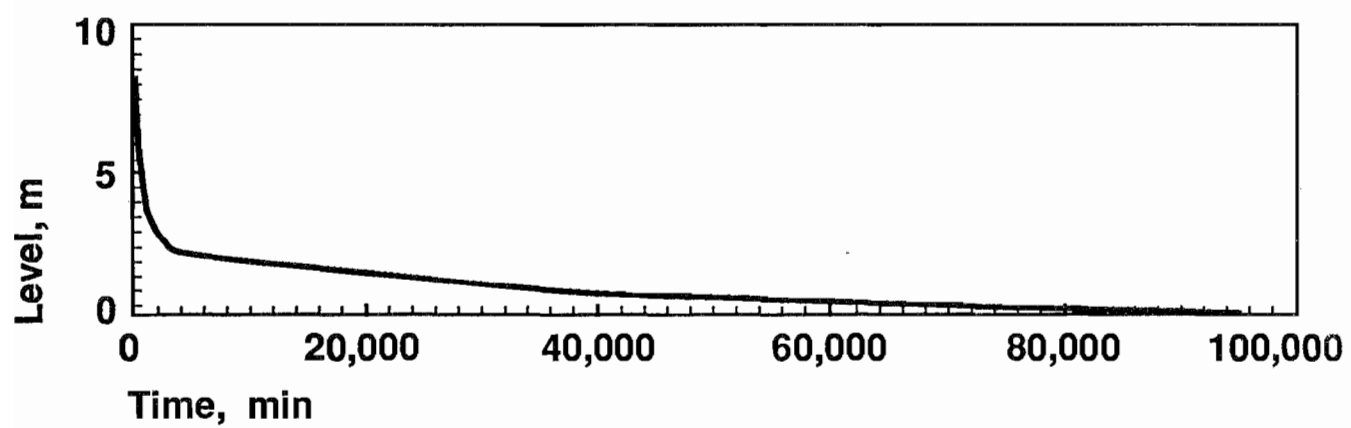


Figure 13. Tracer level in the stope during test 3.

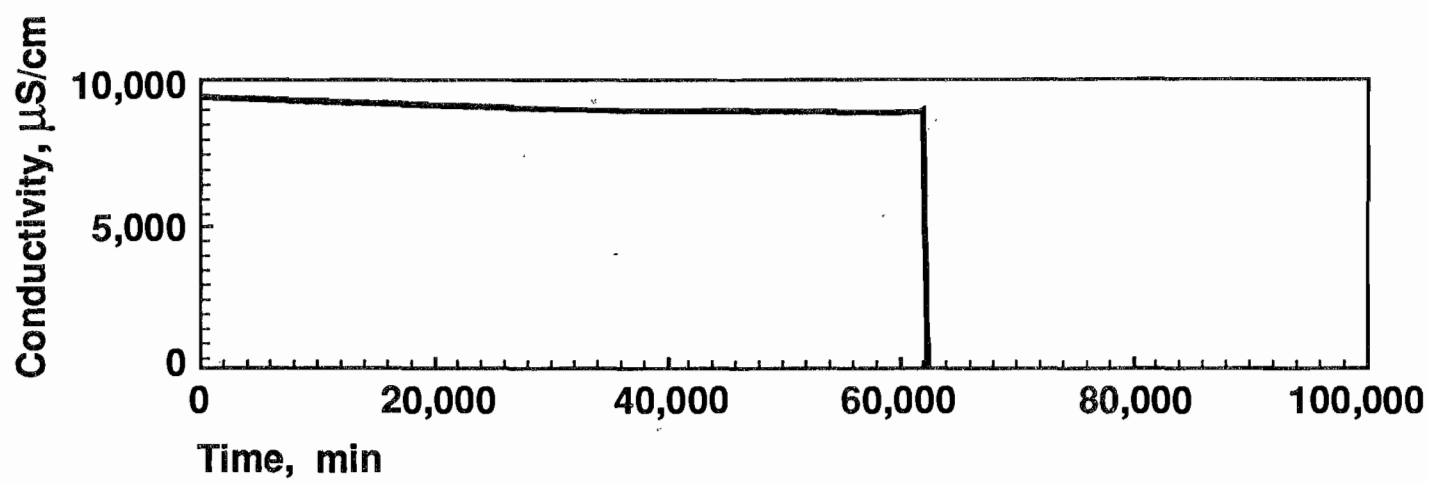


Figure 14. Borehole 4 conductivity during test 3.



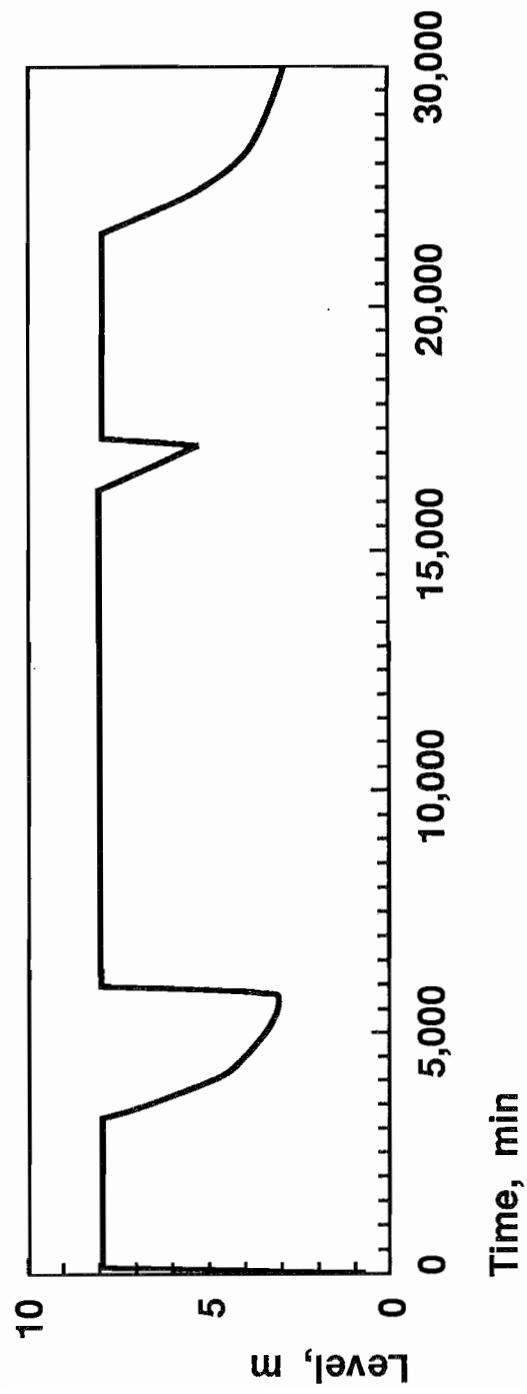


Figure 15. Tracer level in stoep during the constant head test.

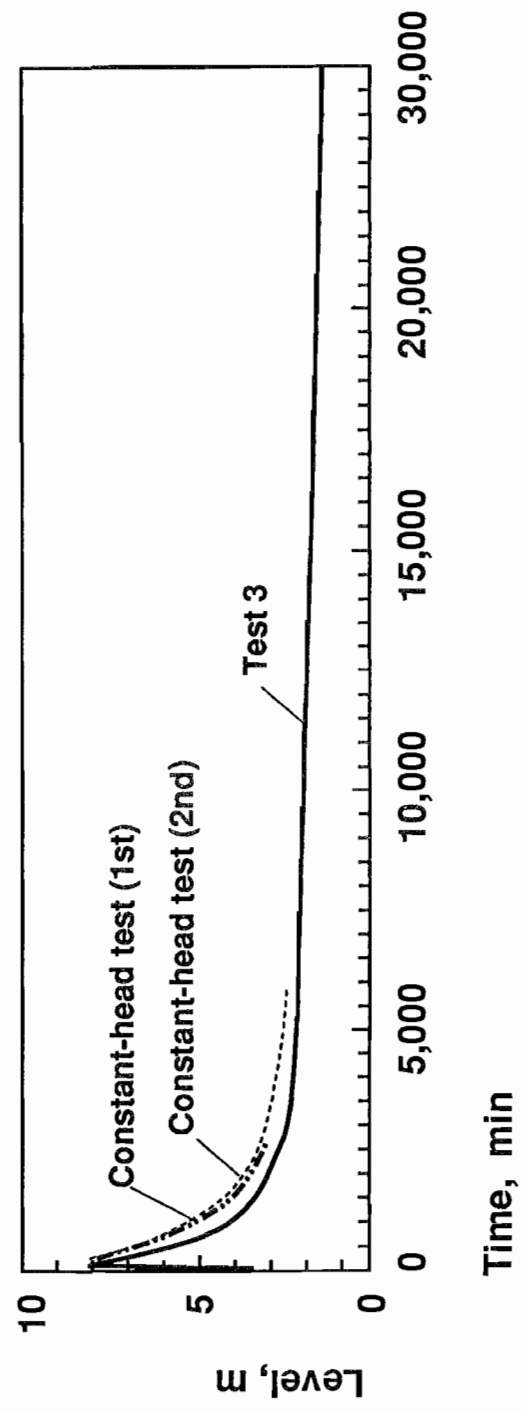


Figure 16. Draining profiles from slope during test 3 and the constant head test.

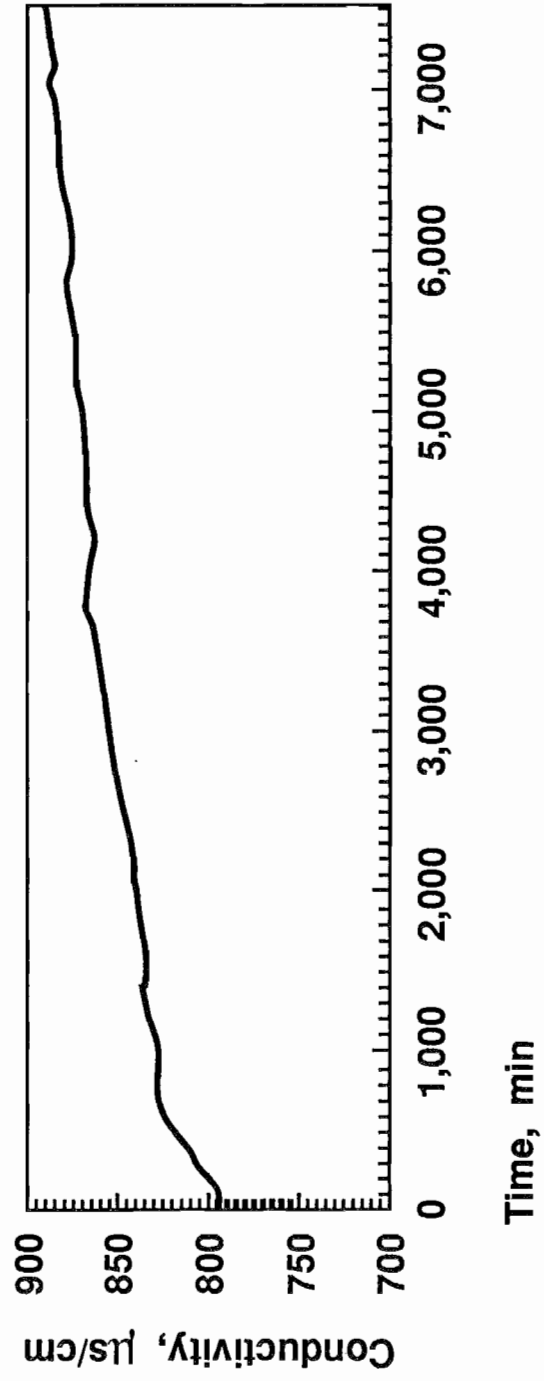


Figure 17. Borehole 3 conductivity during the constant head test.

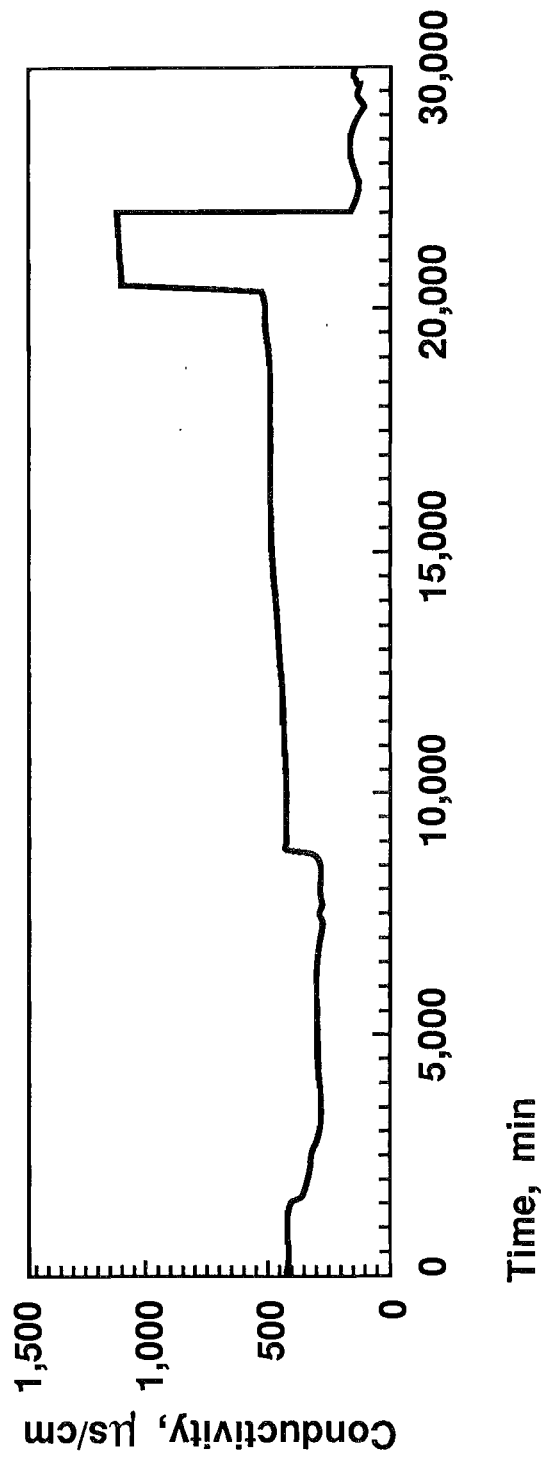


Figure 18. Borehole 4 conductivity during the constant head test.

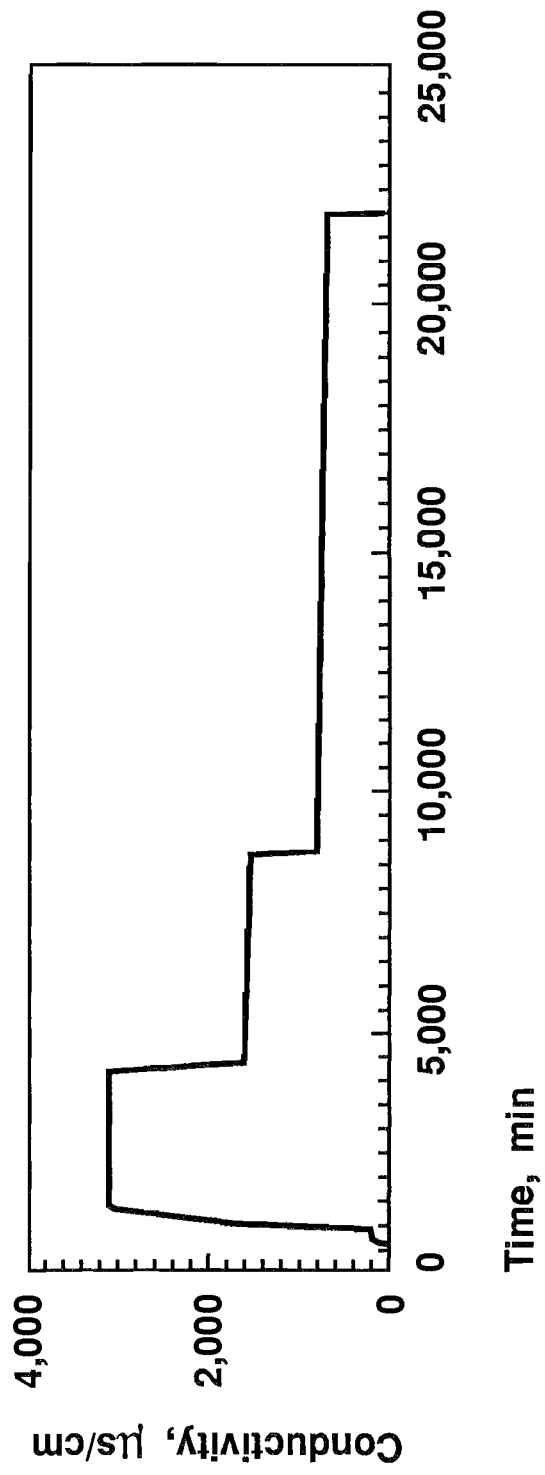


Figure 19. Borehole 6 conductivity during the constant head test.

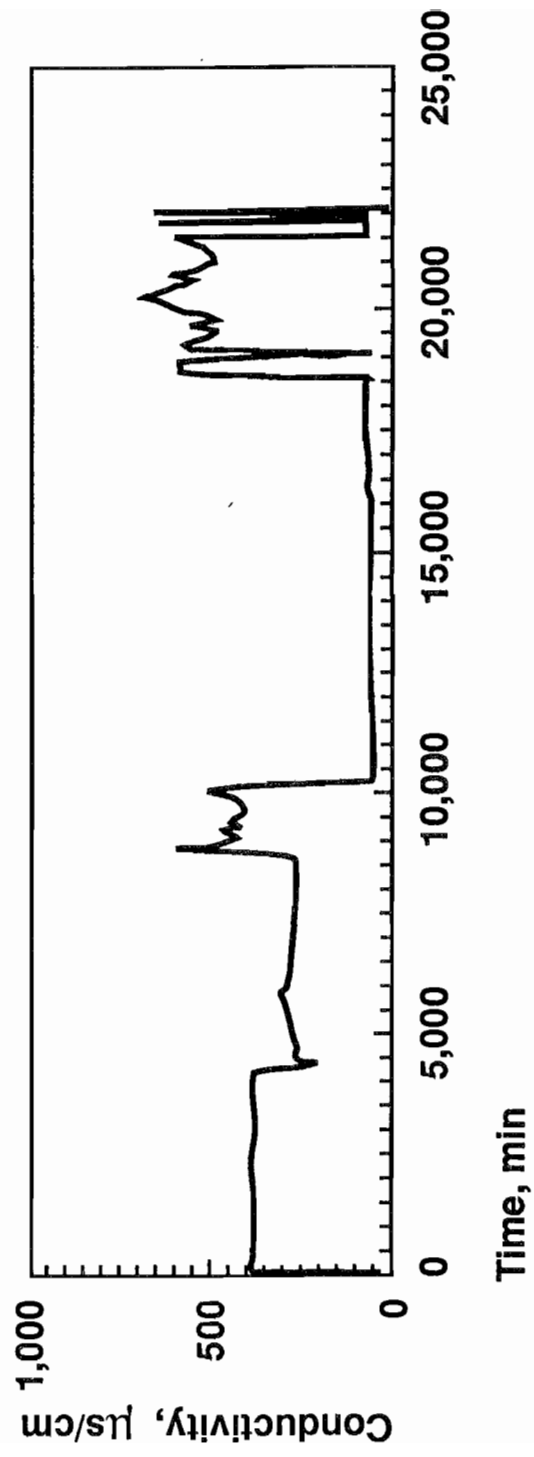


Figure 20. Borehole 8 conductivity during the constant head test.

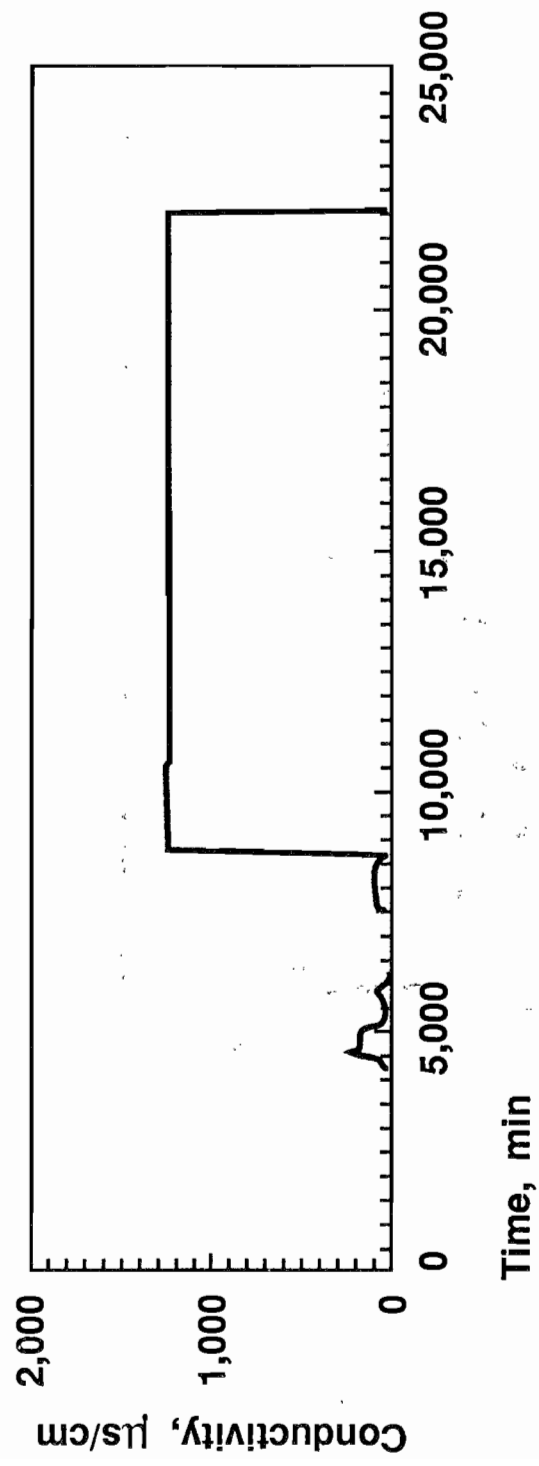


Figure 21. Borehole 10 conductivity during the constant head test.

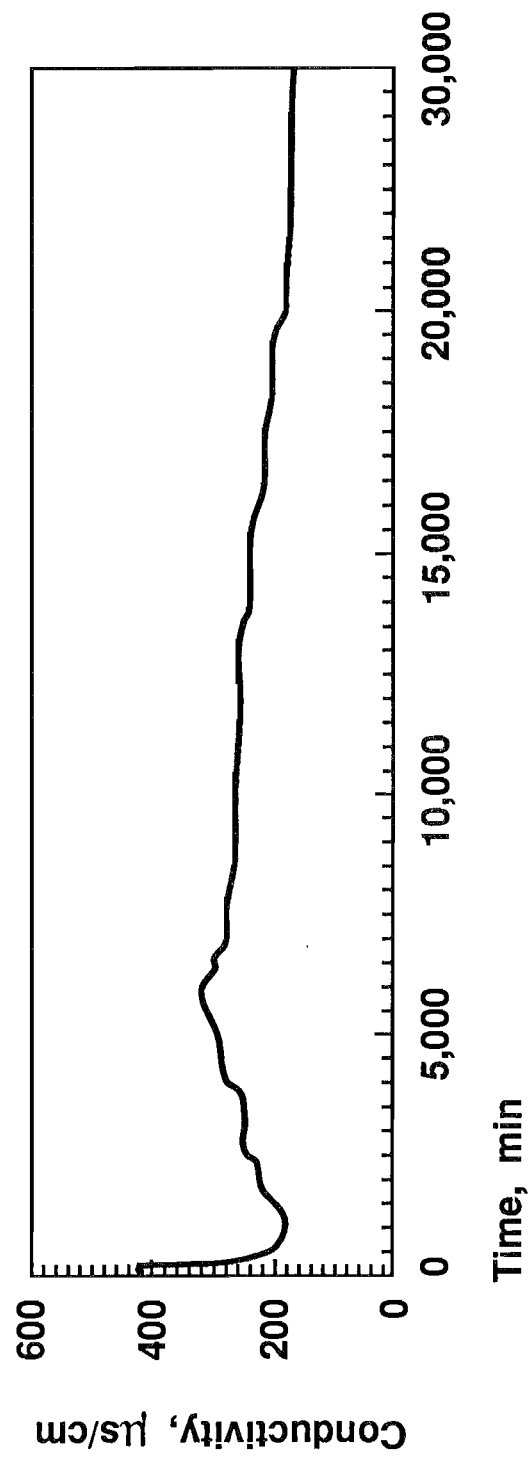


Figure 22. Stope conductivity during the constant head test.